Academy of Sciences of the Czech Republic
Institute of Microbiology
Department of phototrophic microorganisms

What can we learn from Thermoimaging of plants?

Radek Kaňa

Institute of Microbiology, ALGATECH
Department of Phototrophic Microorganisms
Třeboň, Czech Rep.

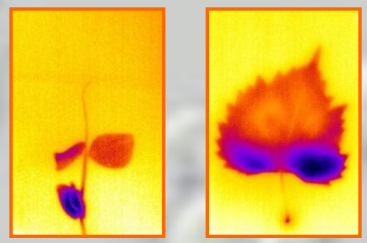

EPPN Summer school, Szeged 2013

MARIE CURIE ACTIONS

Intro2 & BRC

Molecular stress & photobiology group

Temperature detection

Liquid thermometer

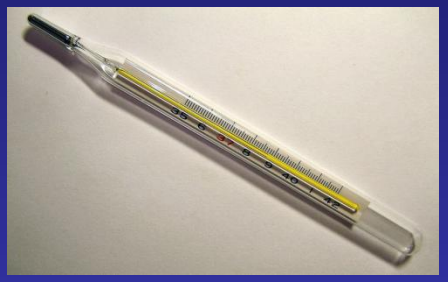

Bi-metallic

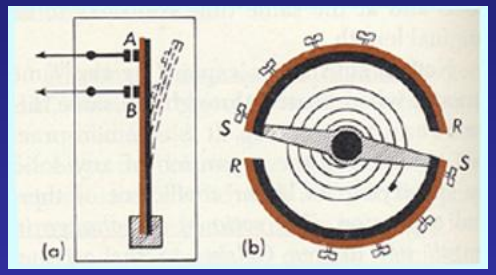

mechanical displacement

Thermistor

Resistance
$\Delta R \sim k\Delta T$

Thermocouple

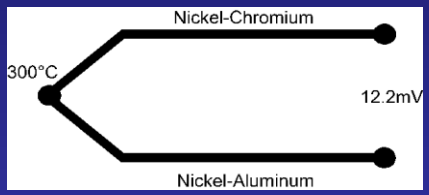

junction between two metals generates a voltage
$\Delta T \sim \Delta U$

INFRARED THERMOMETERS

- *measure temperature using blackbody radiation emitted from objects*
- *non-contact thermometers*

(1) Spot Infrared Thermometer

(2) THERMOGRAPHY

- measurement spatial distribution of temperature over wide areas by thermocamara

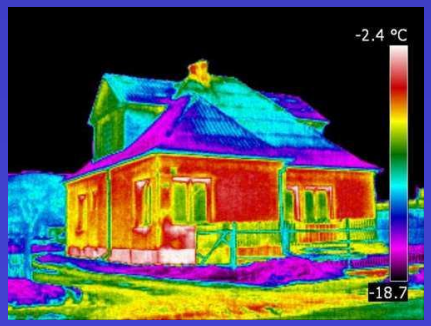

Thermography and plants

A. Measurement of stomatal conductance
B. Water status of leaves detection
C. Biotic stresses detection
D. Mutant selection
E. Thermogenesis of plant tissue
F. Photosynthesis research
G. Plant phenotyping

Black-Body radiation

- Every object emits electromagnetic radiation is directly related to their temperature (Black body concept)
- Radiation of black body object is function of emissivity (ε) and temperature (T) according

Planck radiation formula

$$I(\lambda, T) = \frac{2hc^2}{\lambda^5} \frac{1}{e^{\frac{hc}{\lambda k T}} - 1}$$

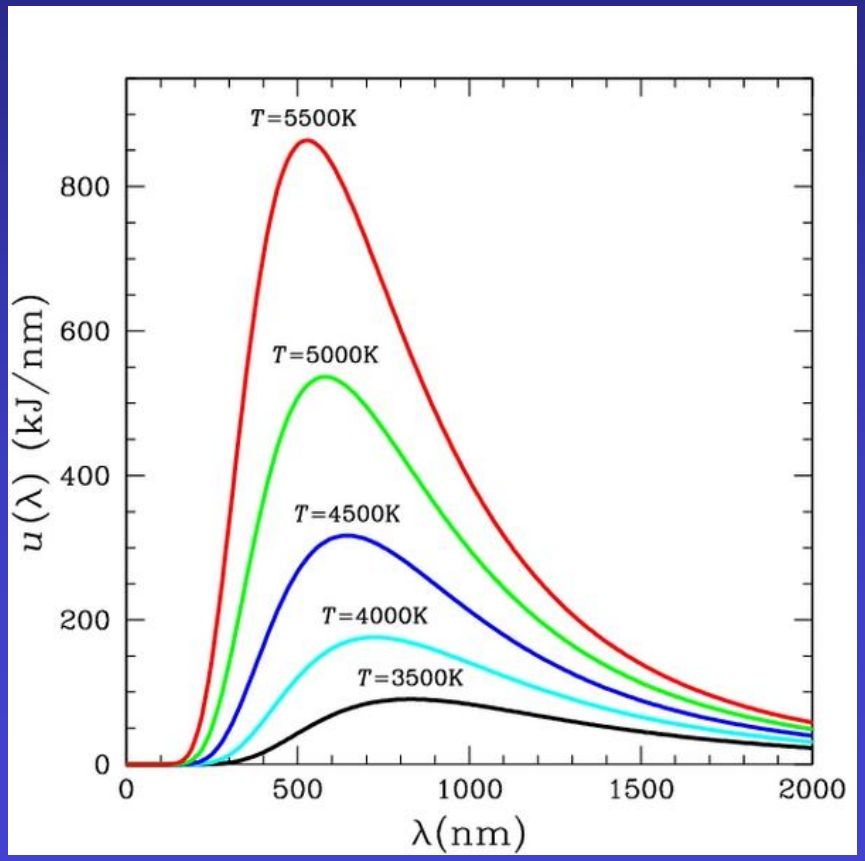

Black-Body radiation

(1) Wien's displacement law – characterize peak of the emission at given [m, K]

(300 K - peak of black body radiation at 10 µm)

$$\lambda_{max} = \frac{2.898 * 10^{-3}}{T}$$

(2) Stefan-Boltzman Law – total energy radiated per unit surface area [W m^{-2}]

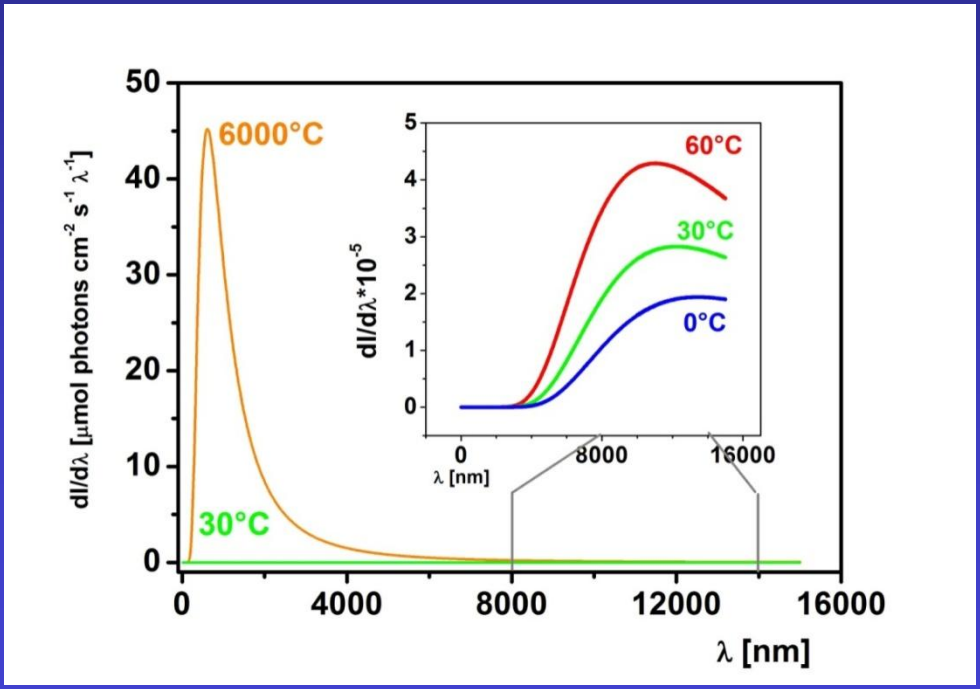

$$R = \varepsilon \sigma T^4$$

Detection of temperature from radiation measurement

- True black body ε = 1
- Real object ε < 1 (ε = 0.92-0.99 for leaf)

	Emissivity
Plant leaves	0.95 (0.92–0.99)
Plant canopies	0.98–0.99
Dry leaves	0.96
Dry grass	0.88
Wood	0.90
Bark	0.94–0.97
Dry soil	0.92
Wet soil	0.95
Sand	0.87–0.92
Distilled water	0.96
Water	0.98–0.99

Thermography – principles 1

- Maximal infrared radiation (based on Wien's replacement law)

$$\lambda_{max} = \frac{2.898 * 10^{-3}}{T}$$

- **Atmospheric window** (minimal absorption of air) between 3-5µm or 8-14µm

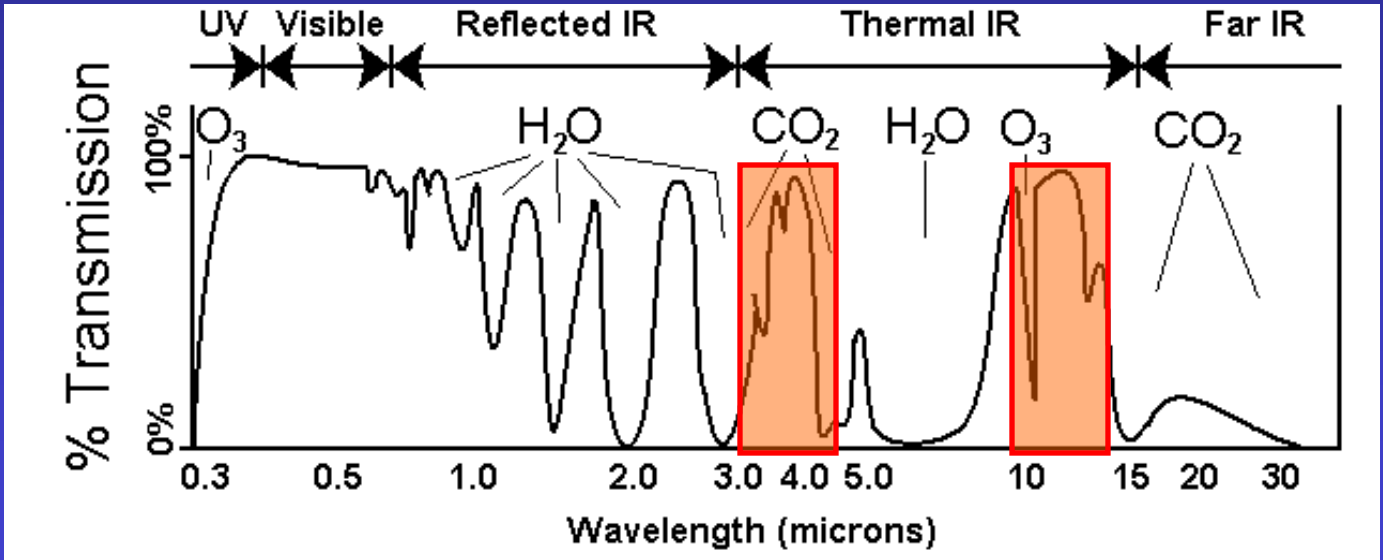

Used wavelengths

Thermography – principles

Thermocamera detects radiation is a sum of object (R_e), background (R_e) and air path (R_e) radiation

1 – direct radiation of measured object (R_e,T)
- reduced with distance
- Function of object temperature

2 – reflected background radiation (R_A,T_b)
- Function of amb. temp T_A

3 – radiation of air path (R_p,T_p)
- Function of path temp T_p

$$R_e \sim \varepsilon_o * \tau_p * P(T_o, \lambda) \text{ with } \tau_p = e^{\frac{-ap*distance}{1000}}$$

$$R_A \sim (1-\varepsilon_o) * \tau_p * P(T_A, \lambda)$$

$$R_p \sim (1-\tau_p) * P(T_p, \lambda)$$

Scheme of radiation pathways

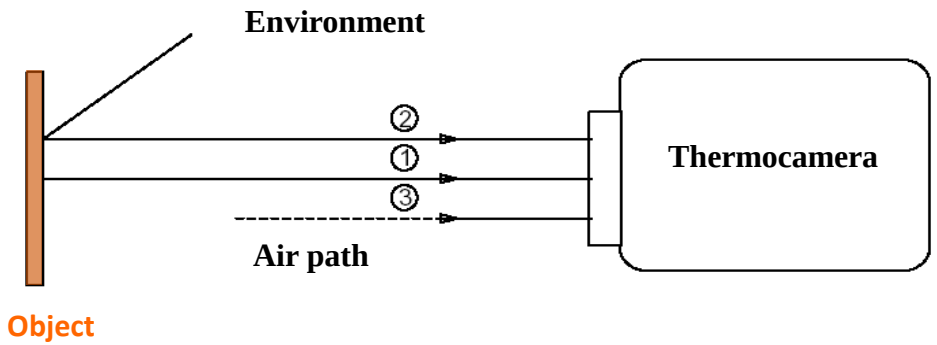

$$R = R_e(T) + R_p + R_A$$

Detection of radiations from object (R_e) with given temperature (T)

Thermal Cameras

Detector type

- *Uncooled detectors*
  - pyroelectric materials like Vanadium oxide
  - Lower sensitivity
  - Faster start of camera
- *Cooled detectors*
  - Semiconductor materials like **HgCdTe –** Mercury-cadmium-telluride
  - Higher sensitivity
  - Cooling range 4-110K
  - Slower start of camera because of cooling

Detector arrangement

- *Object scanning*
  - *Varioscan* by Jena Optic
  - Higher sensitivity
  - Lower frame rate
- *Array of detectors*
  - e.g. Thermovision by FTIR systems
  - Lower resolution, higher frame rate

Cooling system

- *Liquid nitrogen, Helium*
- *Stirling Cooling*

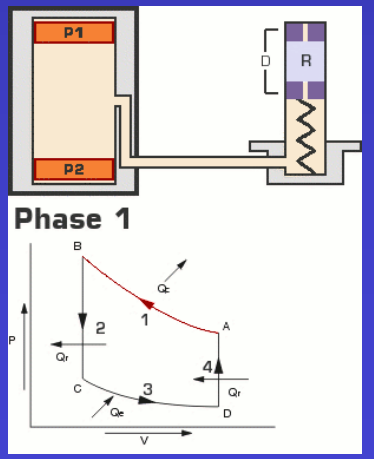

Varioscan 3200

- Producer infratech (optic by Jenoptik)
- Principle of object scanning - image size 360x240 pixels
- Chopper, vertical and horizontal scanner (mirrors)
- Germanium lenses, silicon-germanium (anti-refraction coated)
- Detection at 8-12mm (one MCT detector)
- Sterling-cooled detector (or nitrogen)
- Geometrical resolution of 1.5 mrad with 30 x20 maximal field of view
- Temperature resolution – 0.03K (high resolution camera)
- Absolute accuracy < ±2K
- Frame frequency 1Hz (for 360x240 image)
- Electro-optical zoom (reduction in field view), maximal 6x

InfraTec

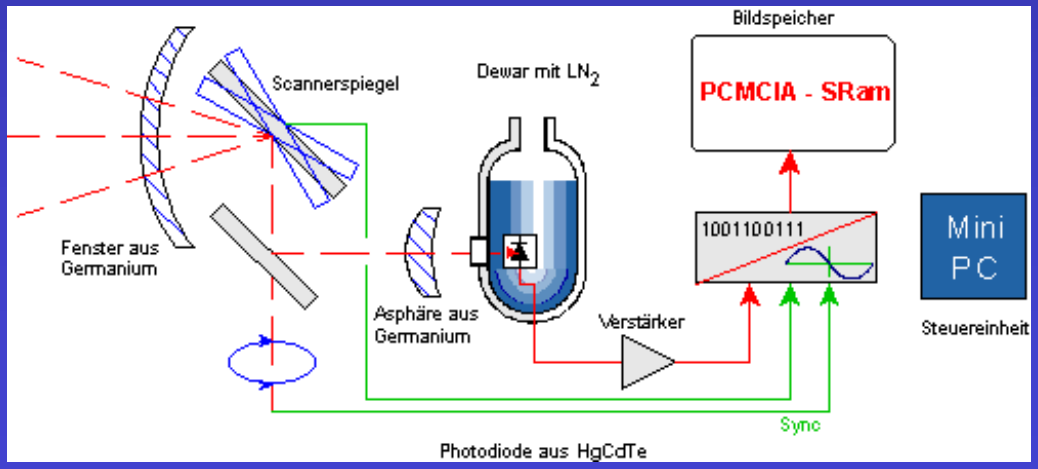

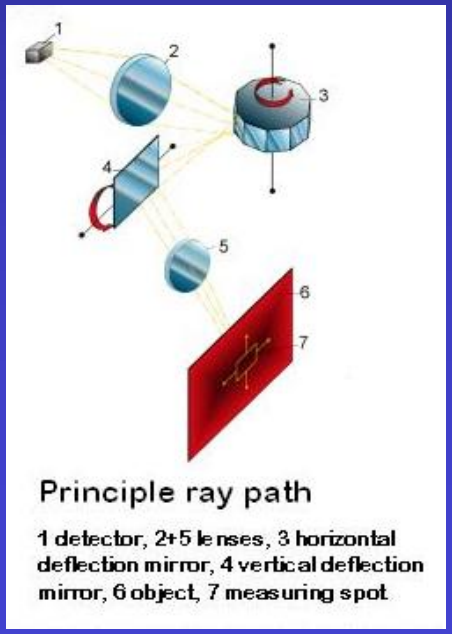

Fast kinetic measurement of "leaf heating" – line scan

- Simple kinetic of leaf heating in ms time scale
- Effect of different rate of leaf heating for functional and non-functional photosynthesis

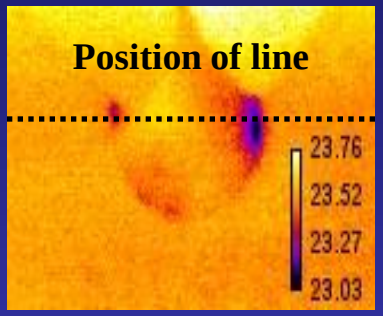

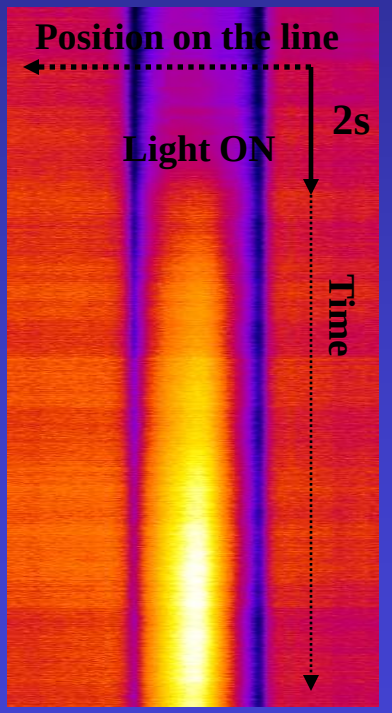

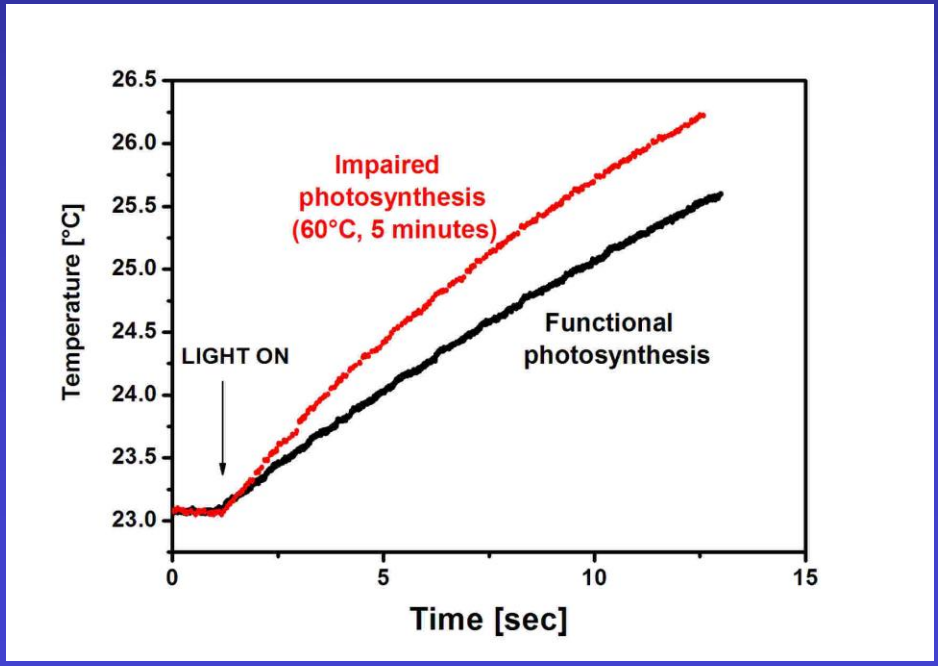

Thermopicture - Image processing

- **Thermoimage** - One channel date with each pixel corresponding to a particular temperature
- Data are stored as matrix with temperature values
- Size of matrix is based on the resolution of thermoimage
- Temperature of particular pixel - value gray in the particular pixel
- Representation of picture by false colours – better visibility

Matrix of temperatures in pixels (10x10)

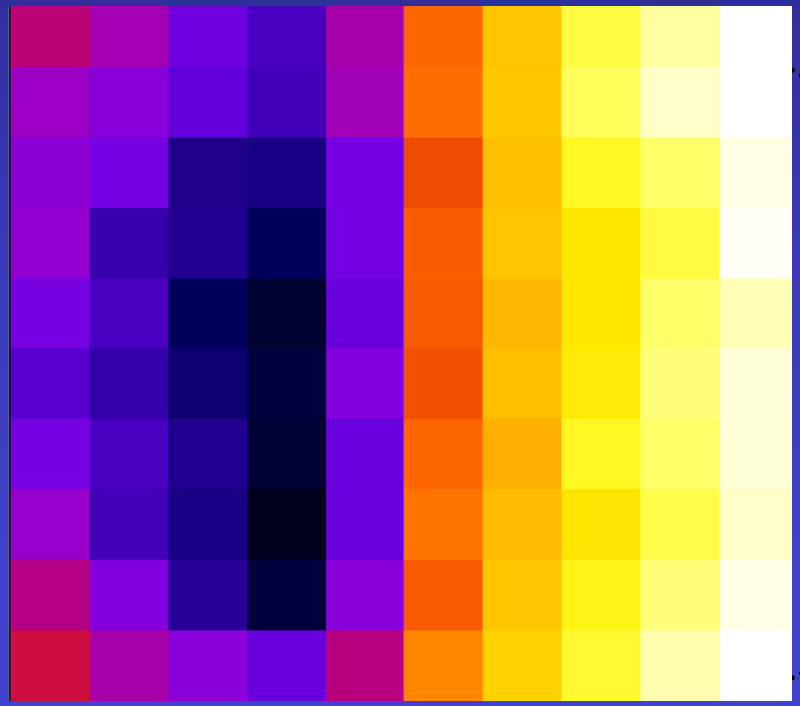

Thermopicture

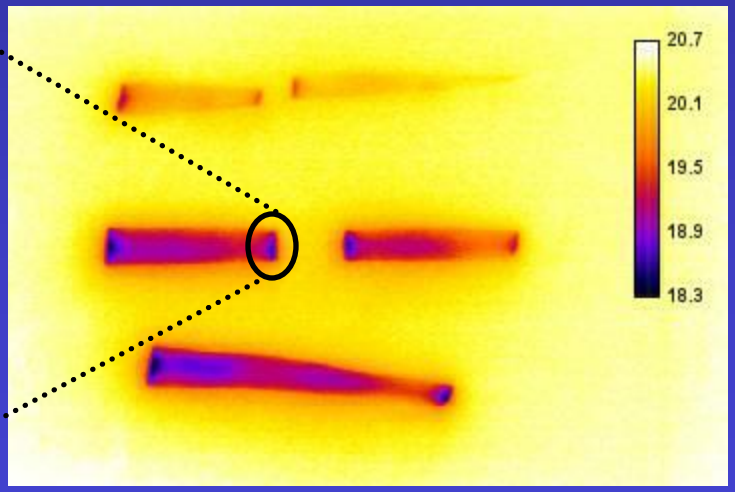

Spatial resolution of thermocamera

- Spatial resolution is greater for thin leaves because of their smaller lateral conductivity
- Thicker leaves are more limited in detection of spatial distribution of stomatal conductance
- Blurring effect due to lateral thermal diffusion (higher for thicker leaf)
- Scattering of radiation from pixel for long distance measurement
- changes optical field of view is changes by electro-optical zoom

Width of camera image

$$w = 2z \tan(\alpha/2)$$

a – angle of camera view
w - width of the imaged area
z - object distance
n – number of pixels

Pixel size

$$p = \frac{w}{n}$$

Field of view

Zoom Step	FOV [°H x °V]
1	30 x 20
2	21 x 14
3	15 10
4	8 x 5
5	5 x 4
6	freely selectable

Blurring effect

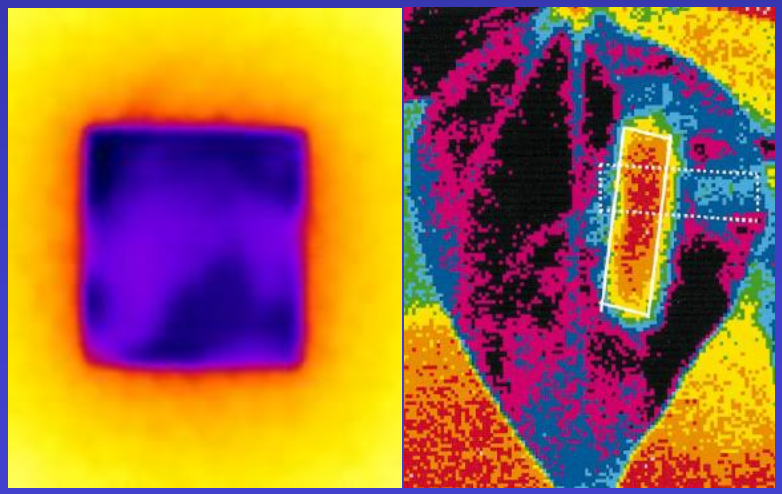

Thermography and plants

A. Measurement of stomatal conductance
B. Water status of leaves detection
C. Biotic stresses detection
D. Mutant selection
E. Thermogenesis of plant tissue
F. Photosynthesis research

Energy balance of leaf

All applications of thermal imaging are based on ***energy balance of leaf*** that characterizes energy fluxes in the leaf per leaf area

Leaf cooling - Transpiration
- Photosynthesis
- Convection and conduction of heat

Leaf heating - Thermogenesis (metabolic processes)
- Irradiation

$$R_n + M - \lambda E - C = \rho_{leaf} c_p l_{leaf} \frac{dT_{leaf}}{dt} = S$$

$R_{n.}$	the radiant flux density absorbed
M	heat produced by metabolism
λE	rate of heat loss through evaporation of water (transpiration)
C	rate of heat loss by conduction or convection to the environment
S	rate of increase of the "heat content" of tissue (ΔT, heat capacity, weight)
ρ_{leaf}, c_p l_{leaf}, T_{leaf}	- density, specific heat, thickness and temperature of leaf
$R_{S.}$	absorbed short-wave radiant flux density
$R_{La.}$	absorbed long-wave radiant flux density
$R_{La.}$	emitted long-wave radiant flux density
$R_{La.}$	emitted fluorescence radiant flux density

$$R_n = R_s + R_{La} - R_{Le} - R_{Fl}$$

Energetic fluxes in the leaf

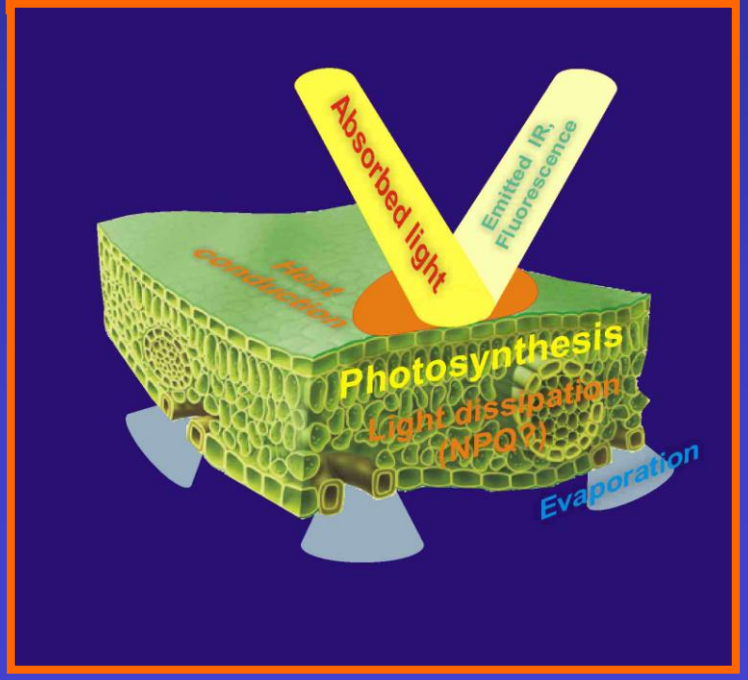

A. STOMATAL CONDUCTANCE

STOMATA - "GATE" for WATER and CO_2

- Stomata are necessary for controlling of CO_2 (for photosynthesis), water content, and temperature
- CO_2 concentration is limited for photosynthesis - bioenergetics issue
- CO_2 and H_2O diffusion proceeds through the stomata formed by two guard cells

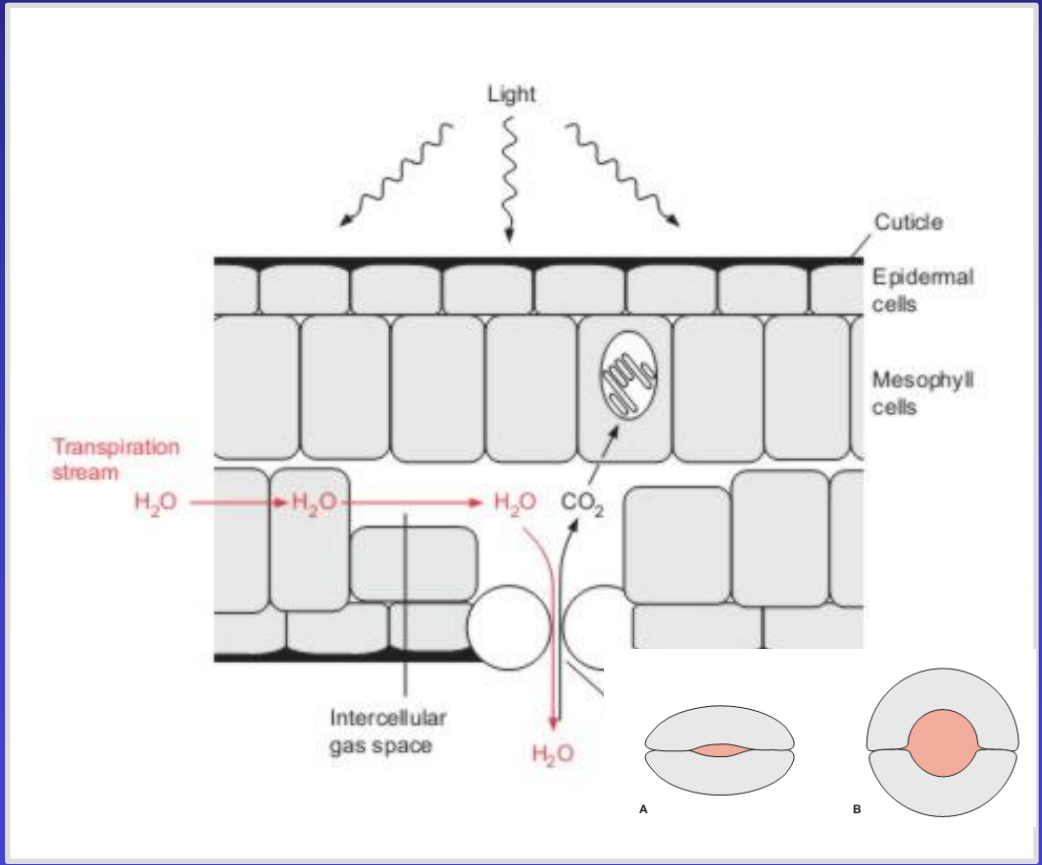

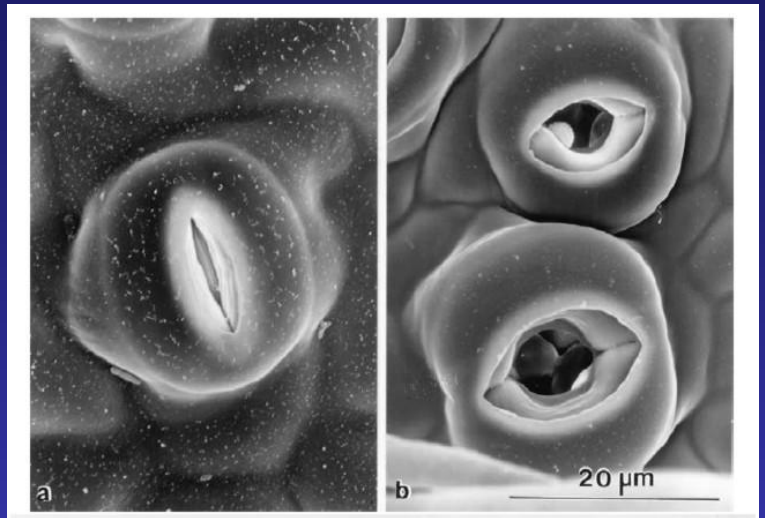

EVAPORATION ON LEAF

Water on leaf surface

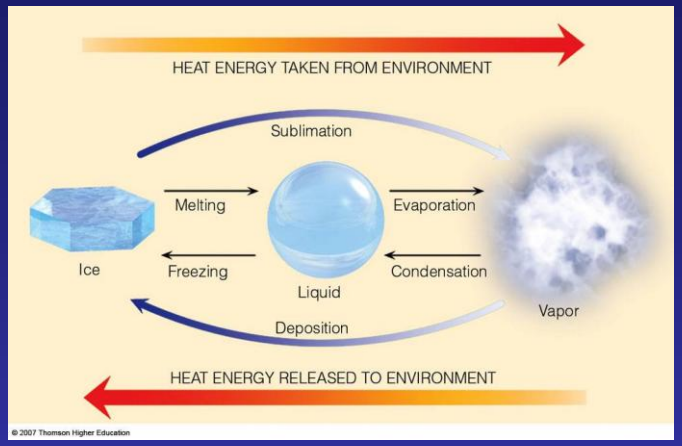

EVAPORATION OF WATER FROM LEAF SURFACE REQUIERS ENERGY

→ IT RESULTS IN DECREASES IN LEAF TEMPERATURE

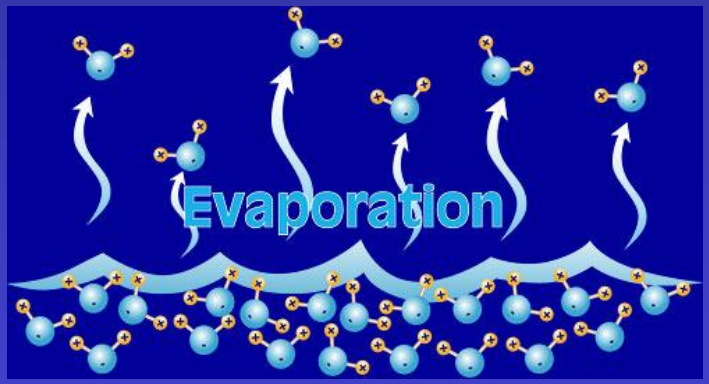

A. STOMATAL CONDUCTANCE

STOMATAL CONDUCTANCE

$$g_s = \frac{(T_{dry} - T_{leaf})}{(T_{leaf} - T_{wet})} \cdot \frac{g_{aH}\ c_p\ g_{HR}}{(c_p\ g_{HR} + g_{aH}\ \lambda\ s/p_a)}$$

Measured parameters

- T_{dry} – covered by Vaseline
- T_{wet} – sprayed by wetting agent (washing up liquid)
- T_{leaf} – temperature of leaf
- u – air velocity (for calculation of r_{aH} …

$$g_{HR} = g_{aH} + g_R$$

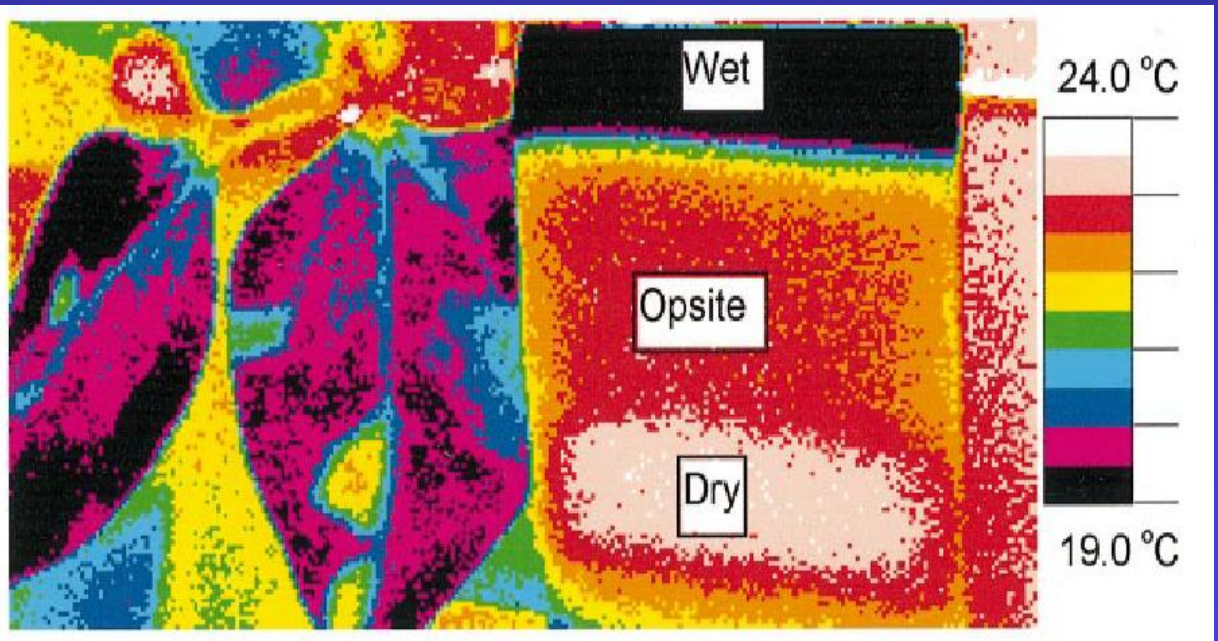

From:Jones 1999 PCE

Known parameters

- g_{aH} - Boundary layer conductance for heat
- g_{HR} - Overall heat conductance in leaf
- g_R - Radiative conductance
- p_a - Atmospheric pressure
- c_p - Specific molar heat of air
- λ – Molar latent heat of water vaporization - (44.1 kJ mol $^{-1}$)
- **s** - Slope of the curve "saturation water vapor pressure to temp."

A. STOMATAL CONDUCTANCE

- Measurements of stomatal conductance (*Jones HG 1999 PCE*) based on temperature changes
- Calculations are based on energy balance equation

STOMATAL CONDUCTANCE

$$g_s = \frac{(T_{dry} - T_{leaf})}{(T_{leaf} - T_{wet})} \cdot \frac{g_{aH}\, c_p\, g_{HR}}{(c_p\, g_{HR} + g_{aH}\, \lambda\, s/p_a)}$$

Standardization of method

- independent measurement of **boundary layer** properties has to be done
- known conductance of reference surfaces are necessary

Standard surfaces

- Micropores membranes
- Wet surface (sprayed by wetting agent) – no leaf resistance to water
- Dry surface (covered by vazeline) – maximal leaf resistance to water

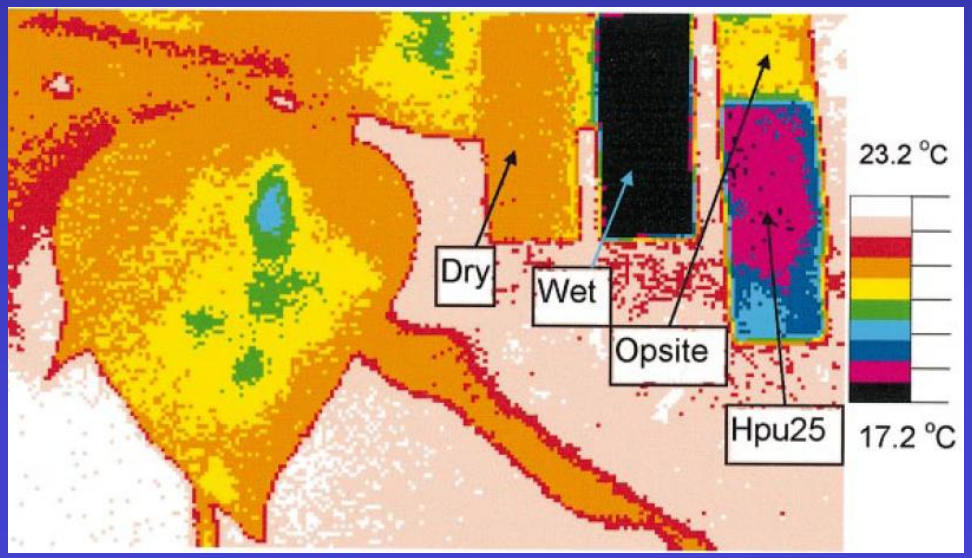

From:Jones 1999 PCE

Conductance to water vapour g_{lw}

	Mean conductance (mmol $m^{-2}s^{-1}$)	Comments
PM2U[a]	900–1300	pore size 5–10 μm
PM3T[a]	680–1000	pore size 2 μm
PM9P[a]	1470–1800	pore size 1 μm
PM28Y[a]	1200–1400	pore size 2·5 μm
Net909[b]	8–12	breathable sticking plaster
Hpu25[b]	450–620	very thin wound dressing material
Opsite[b]	18–25	very thin wound dressing material
Goretex	300–800	microporous membrane bonded to rainwear material

Boundary layer of leaf

- **Thin layer on the leaf surface affecting transfer of heat and gases**

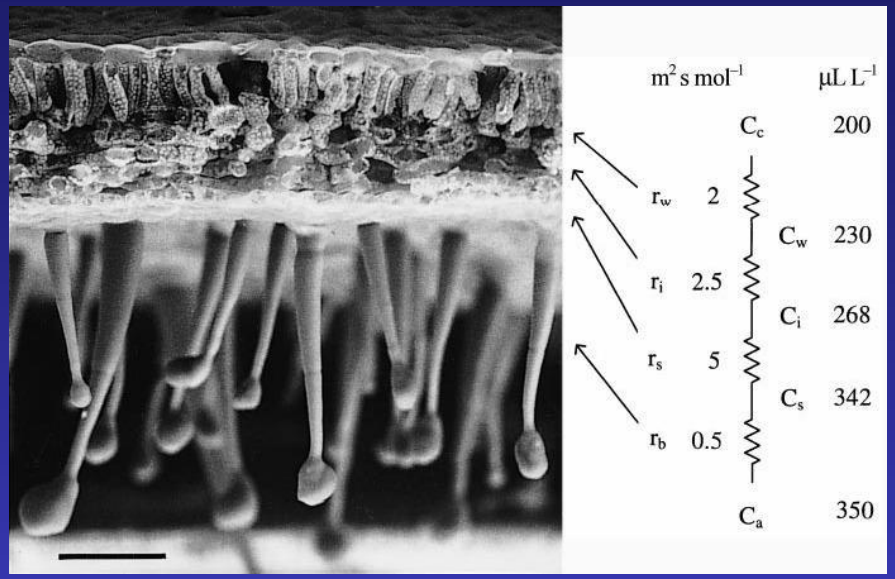

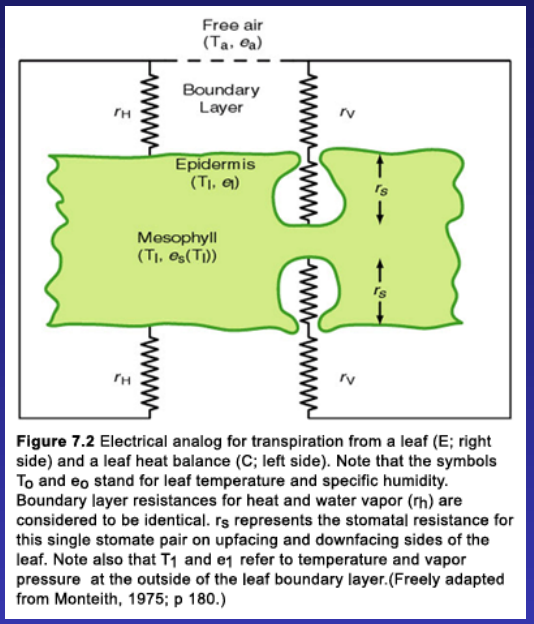

Figure 7.2 Electrical analog for transpiration from a leaf (E; right side) and a leaf heat balance (C; left side). Note that the symbols T_o and e_o stand for leaf temperature and specific humidity. Boundary layer resistances for heat and water vapor (r_h) are considered to be identical. r_s represents the stomatal resistance for this single stomate pair on upfacing and downfacing sides of the leaf. Note also that T_1 and e_1 refer to temperature and vapor pressure at the outside of the leaf boundary layer.(Freely adapted from Monteith, 1975; p 180.)

- Important for function of leaf, Critical for gases and heat transfer
- Type of air transfer is affected by leaf shape, surface, air velocity, trichoms (hairs)
- Parameter of baondary layer are required for calculation of stomatal conductance

Air transfer can be laminar, turbulent or mix (based on Reynolds number) – changes in the heat transfer

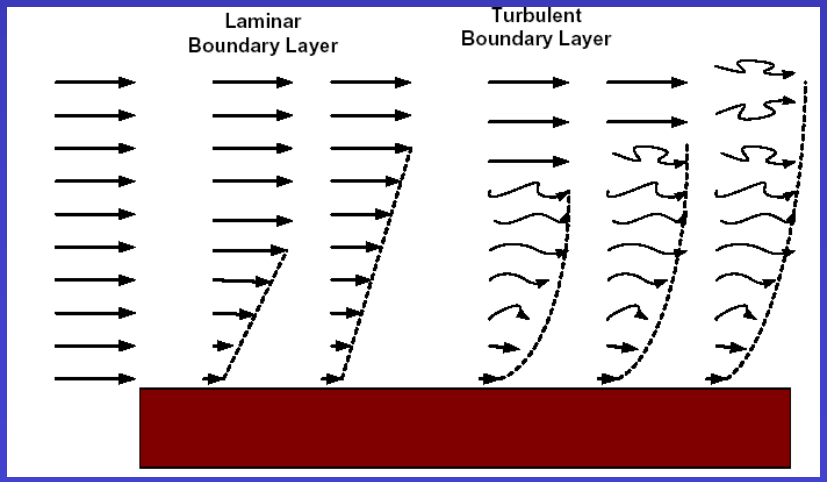

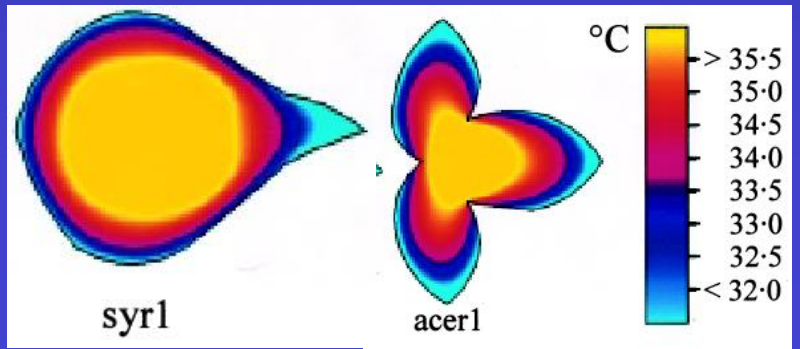

STOMATAL PATCHINESS

- Coherent reas with different stomatal conductance
- collections of tens to thousands of stomata can have similar conductances, different from those of surrounding stomata. This is the phenomenon of "stomatal patchiness."
- It is induced by different stimuls, mechanism is unknown

REAL PICTURE

AVERAGE (e.g. Gas exchange)

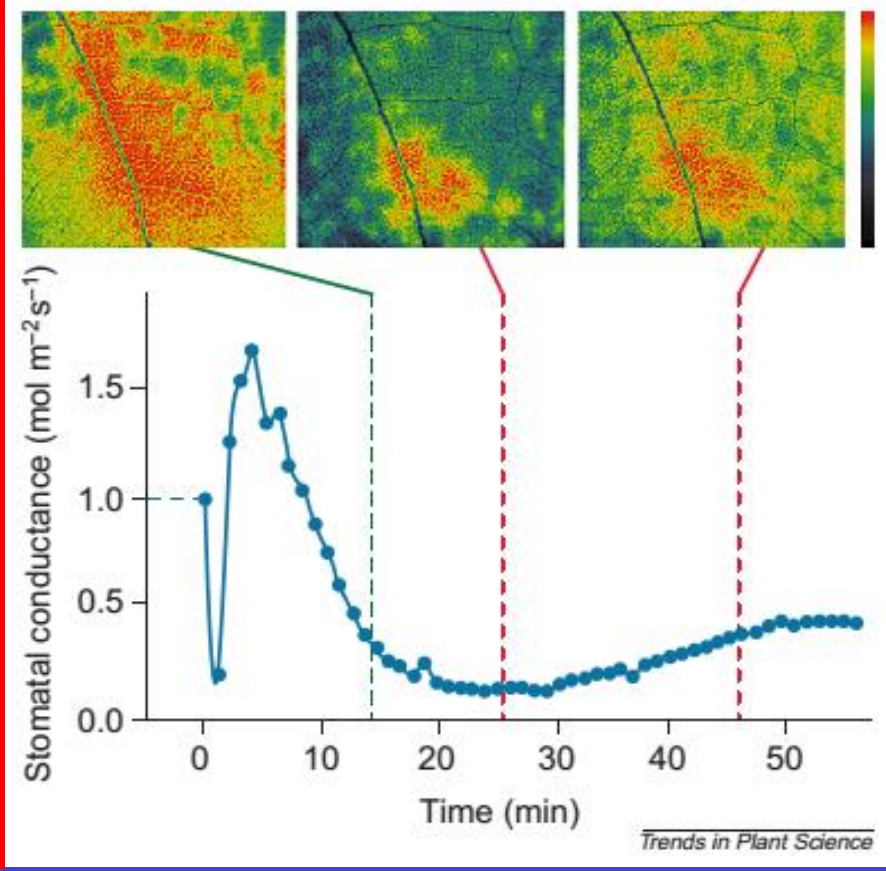

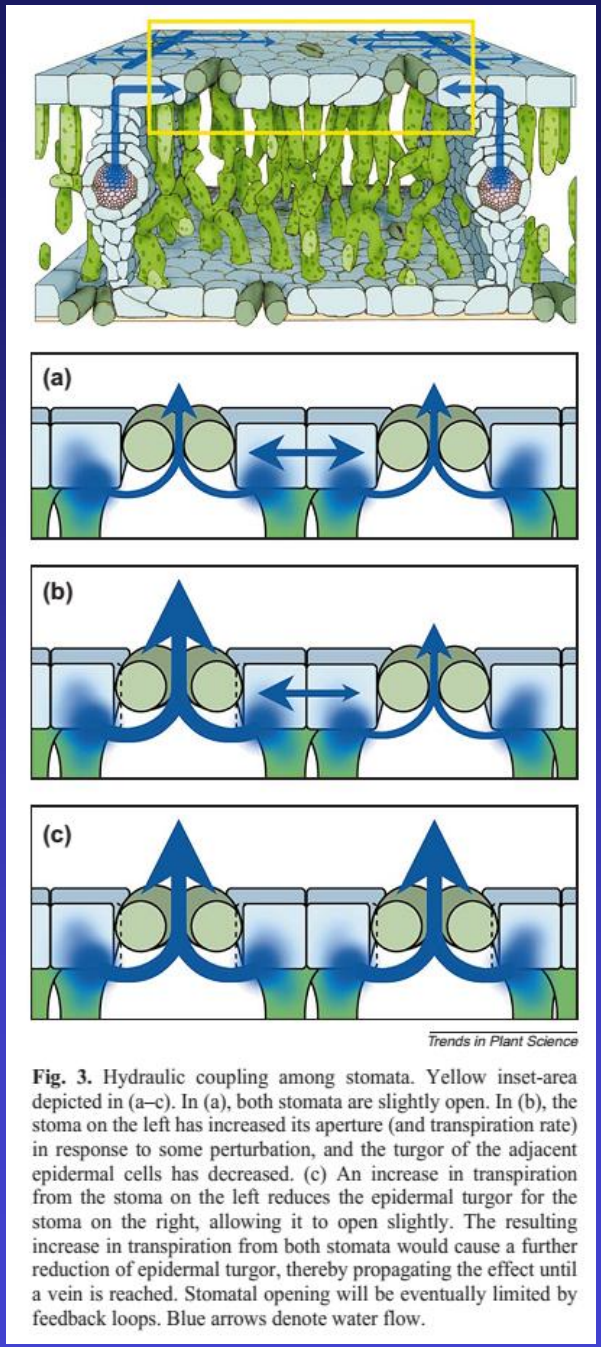

Fig. 3. Hydraulic coupling among stomata. Yellow inset-area depicted in (a–c). In (a), both stomata are slightly open. In (b), the stoma on the left has increased its aperture (and transpiration rate) in response to some perturbation, and the turgor of the adjacent epidermal cells has decreased. (c) An increase in transpiration from the stoma on the left reduces the epidermal turgor for the stoma on the right, allowing it to open slightly. The resulting increase in transpiration from both stomata would cause a further reduction of epidermal turgor, thereby propagating the effect until a vein is reached. Stomatal opening will be eventually limited by feedback loops. Blue arrows denote water flow.

Mott and Buckley 2000 TPS

STOMATAL PATCHINESS

Top row: images of chlorophyll fluorescence from a leaf of Xanthium strumarium following a sudden decrease in ambient humidity at time zero.

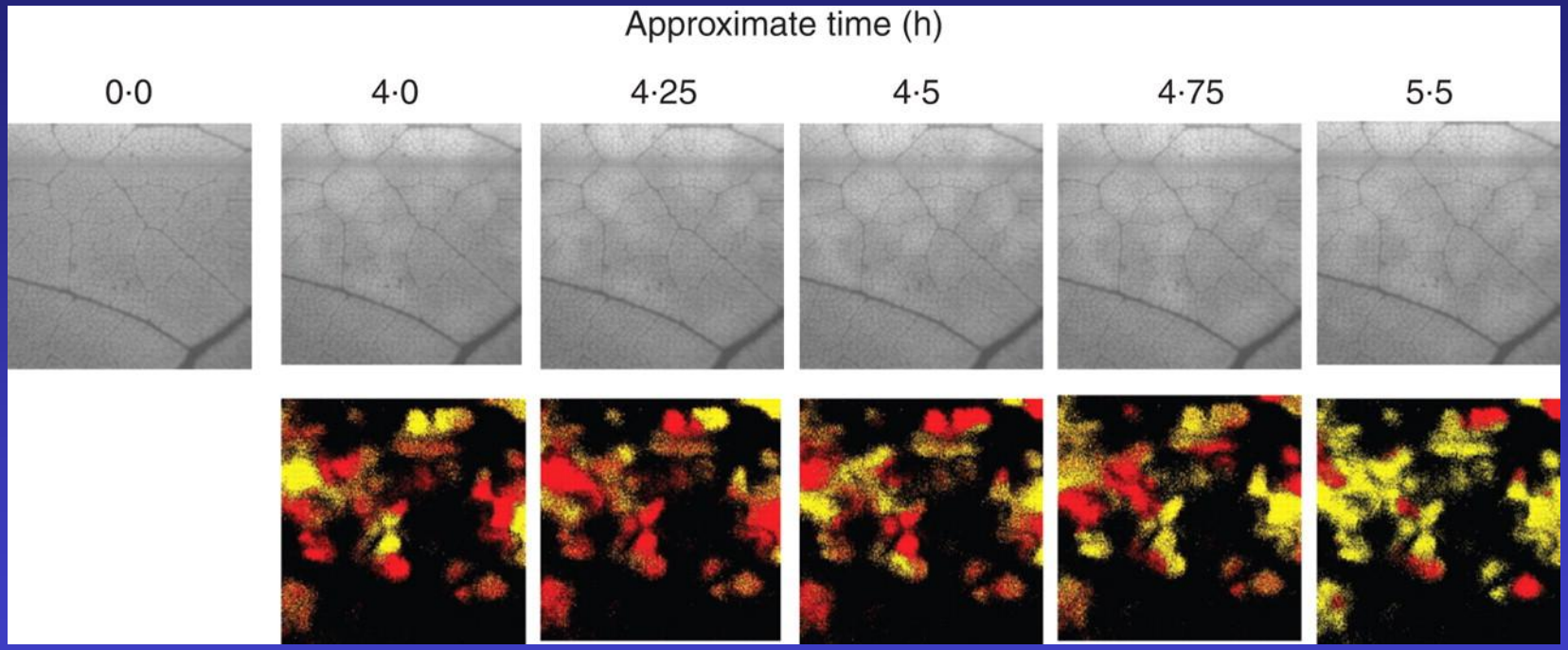

Bottom row: pixels that tend to brighten over a period of a few minutes are coloured red, whereas those that tend to dim are coloured yellow. Pixels showing little change are black.

Mott K A , and Peak D Ann Bot 2007;99:219-226

ANNALS OF BOTANY

STOMATAL PATCHINESS

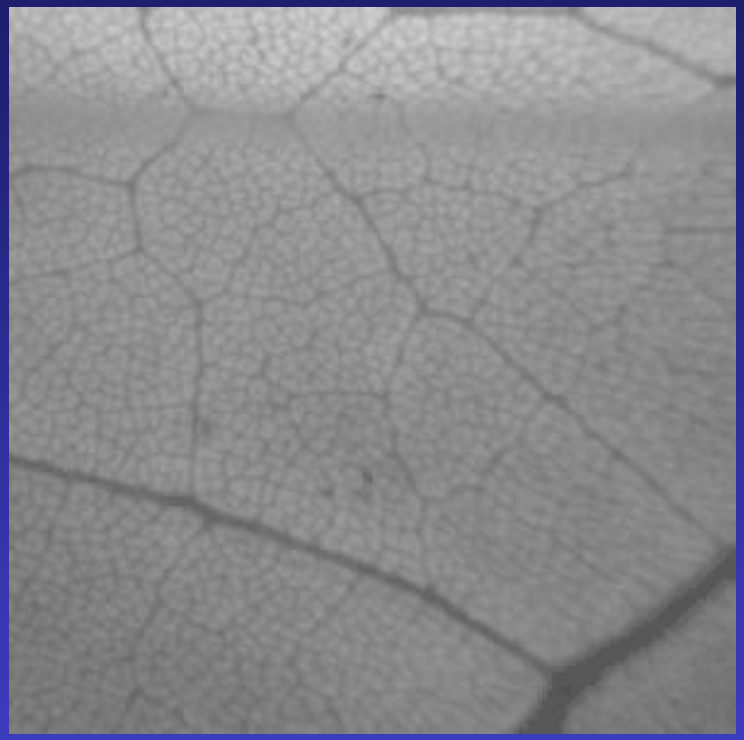

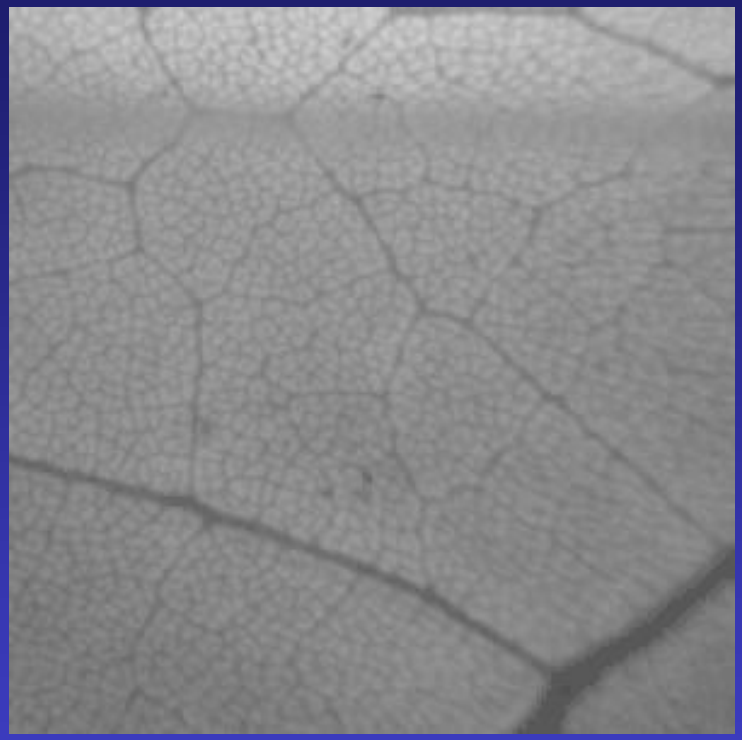

Measured from chlorophyll fluorescence only
(NOT DIRECTLY)

Mott K A , and Peak D Ann Bot 2007;99:219-226

ANNALS OF BOTANY

STOMATAL PATCHINESS - THERMOIMAGING

- Stomatal patchiness observed after reduction in ambient humidity
- Slow movement of stomata patch (20µm s^{-1}), similar chla fluorescence and thermal pattern of movement
- fluorescence patterns were largely the result of stomatal conductance patterns
- both thermal and fluorescence images showed patches of stomatal conductance that propagated coherently across the leaf surface.

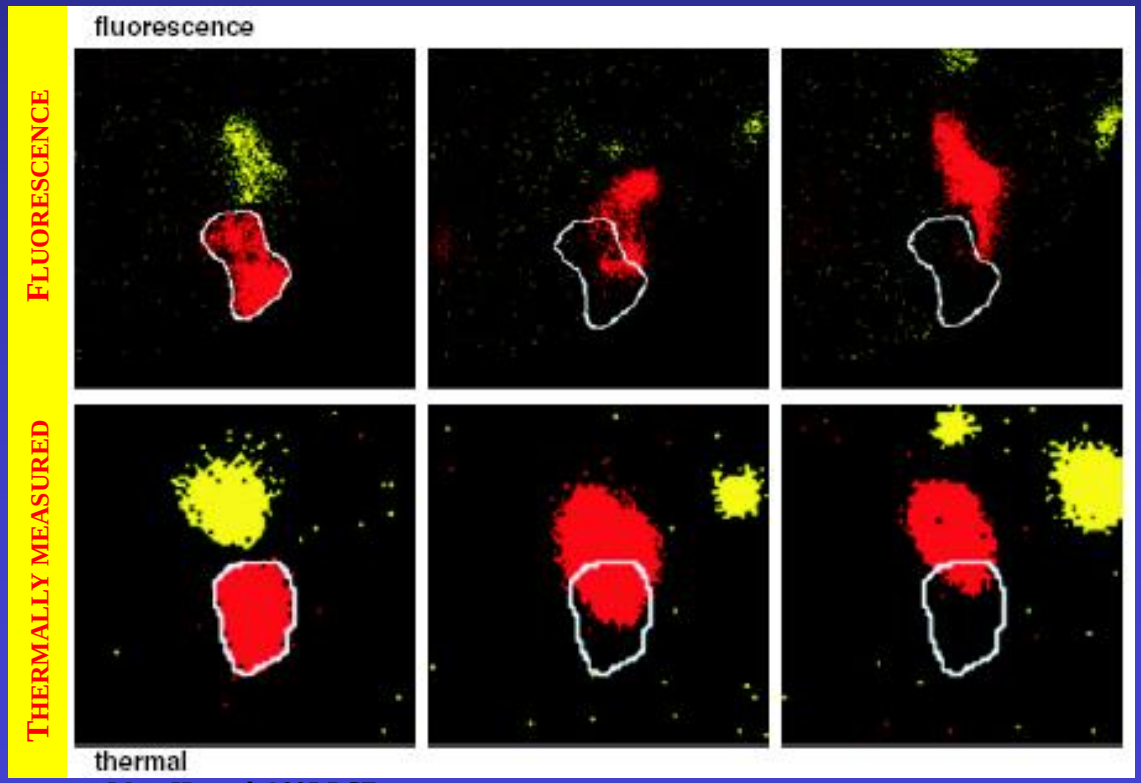

West JD et al. 2005 PCE

B. WATER STATUS OF PLANTS

- Pronounced increase in the leave temperature appears several days after stopping of irrigation at 3rd day of measurement (*Chaerle et al 2005 TBT*)

OPTIMAL IRRIGATION

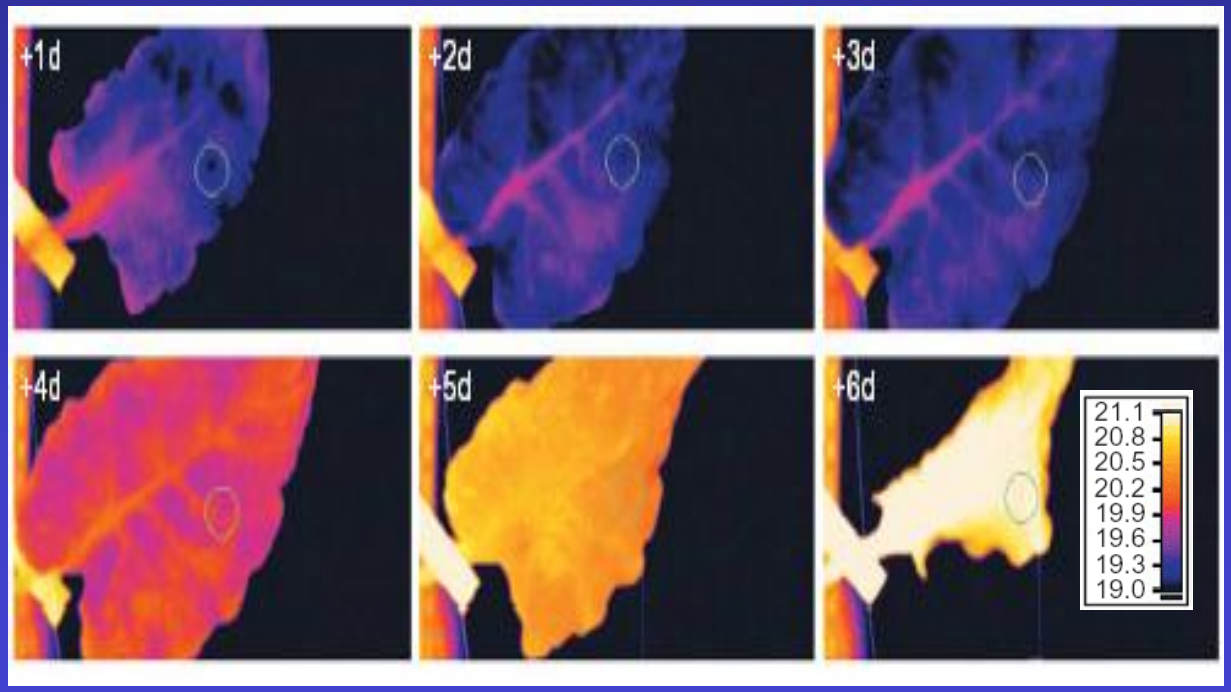

NO IRRIGATION

Chaerle et al 2005 TBT

- Water loss of detached wheat leaves

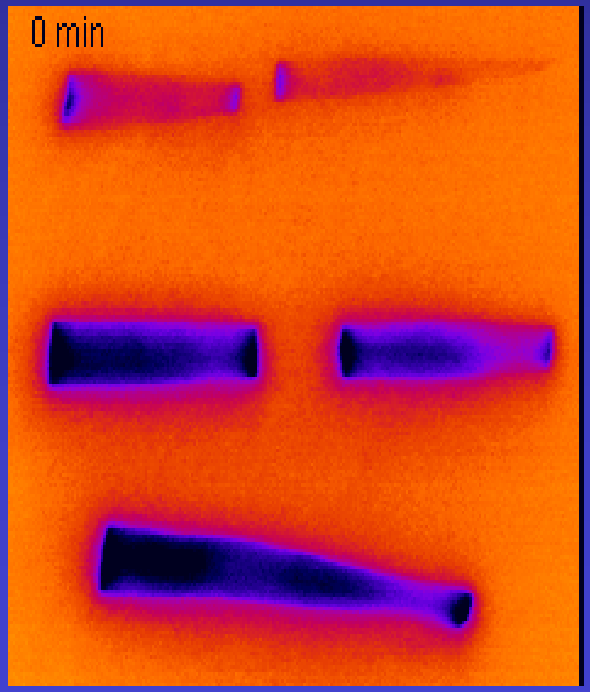

Kaňa - unpublished

B. WATER STATUS OF PLANTS

- Changes in the distribution of temperature can be used as indicator of water stress
- Image classification is necessary (well watered-**W**, dry **D**, **P** measured plant)
- Combination of infrared and visible camera
- Application for plant identification

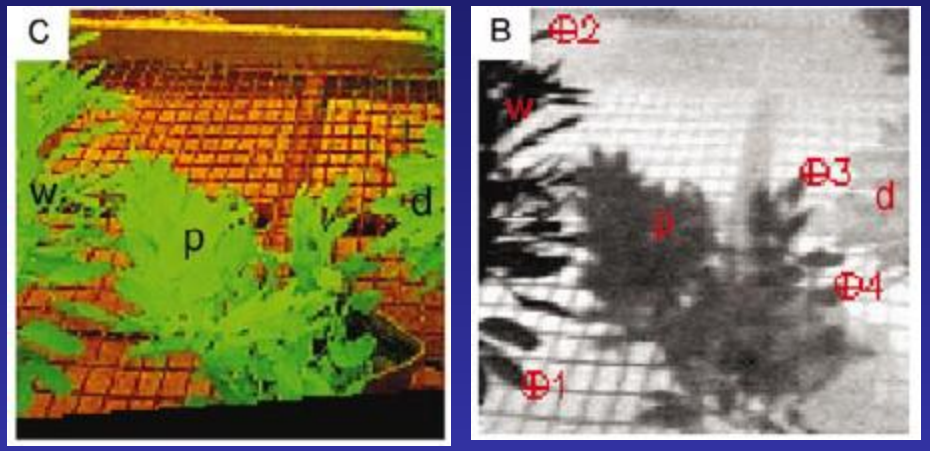

Control (non-stressed) leaf

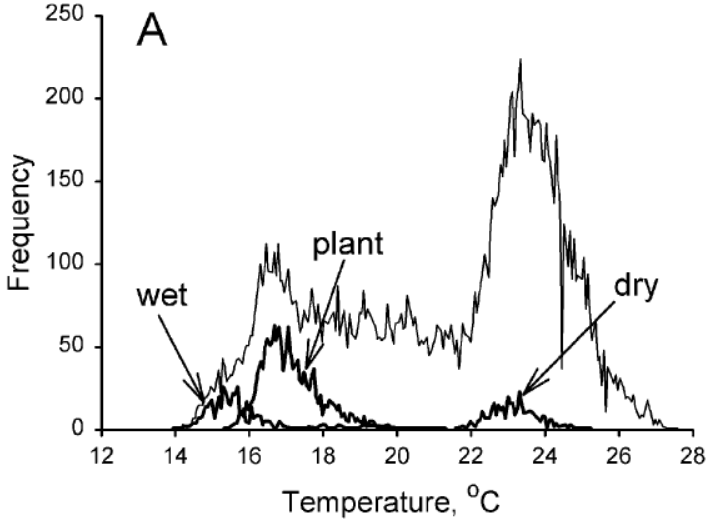

Stressed leaf (non-watered)

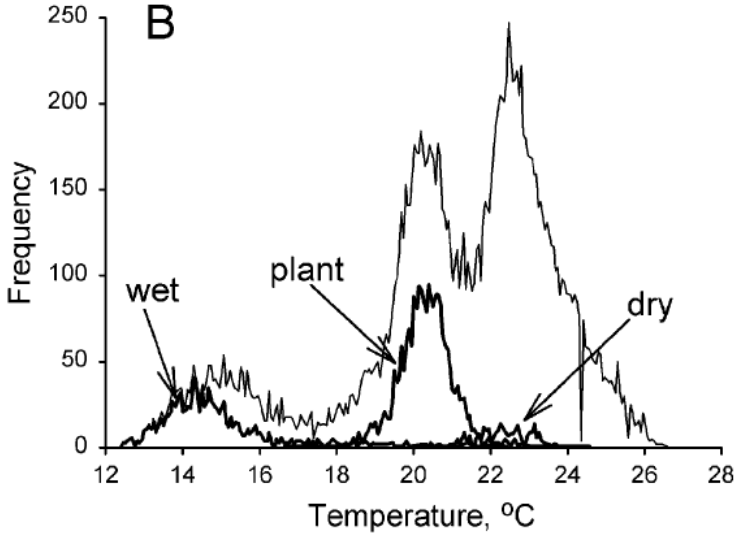

From: Leinonen and Jones 2006 JEB

LEAF WATER POTENTIAL

Water potential quantifies the tendency of water to move from one area to another due to osmosis, gravity, mechanical presure, or matrix effects (e.g. surface tension)

THERMOGRAPHY CAN BE USED FOR ROUGH ESTIMATION OF LEAF WATER POTENTIAL

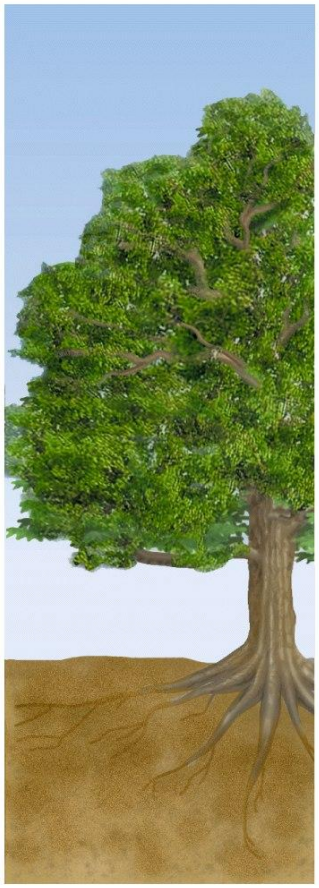

Low water potential
Atmosphere ψ: –95.2 MPa
(Changes with humidity; usually very low)

Leaf ψ: –0.8 MPa
(Depends on transpiration rate; low when stomata are open)

Root ψ: –0.6 MPa
(Medium–high)

Soil ψ: –0.3 MPa
(High if moist; low if extremely dry)

High water potential

Water transport

Figure 36-3 Biological Science, 2/e

$$\Psi = \Psi_0 + \Psi_\pi + \Psi_p + \Psi_s + \Psi_v + \Psi_m$$

- Ψ_0 is the reference correction,
- Ψ_π is the solute potential,
- Ψ_p is the pressure component,
- Ψ_s is the gravimetric component,
- Ψ_v is the potential due to humidity, and
- Ψ_m is the potential due to matrix effects

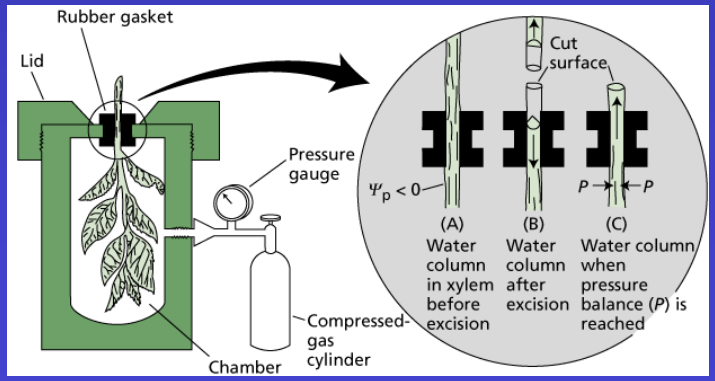

B. WATER STATUS OF PLANTS – STRESS INDICATOR

Crop water stress index (Idso's)

$$CWSI = (T_{canopy} - T_{nws})/(T_{dry} - T_{nws})$$

- T_{nws} – well watered crop
- T_{dry} – non-transpirating crop
- T_{canopy} – canopy
- Standard relationship between T_{canopy}-T_{air} and humidity has been developed for all crops
- Changes in the relative error for different water pressure deficit

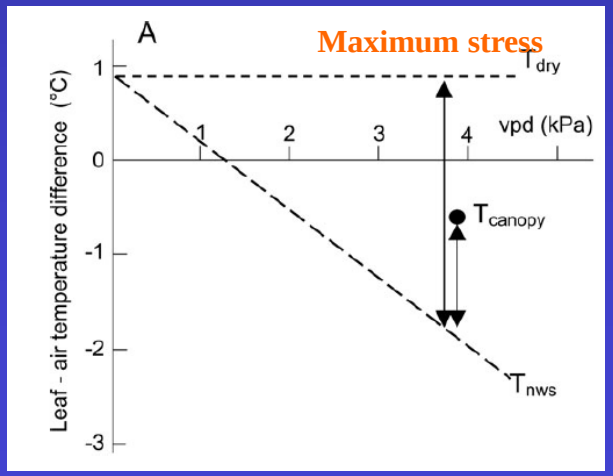

Crop water stess index by Jones

$$SI_{CWSI} = (T_{leaf} - T_{wet})/(T_{dry} - T_{wet})$$

- T_{leaf} – leaf temperature
- T_{wet} – wet surface (with wetting agent)
- T_{dry} – dry surface temp. – with Vaseline
- Based on standard surfaces, for single leaf measurement

Determination of leaf water potential

- Based on on correlation between CWSI ans LWP
- Remote sensing of field water status

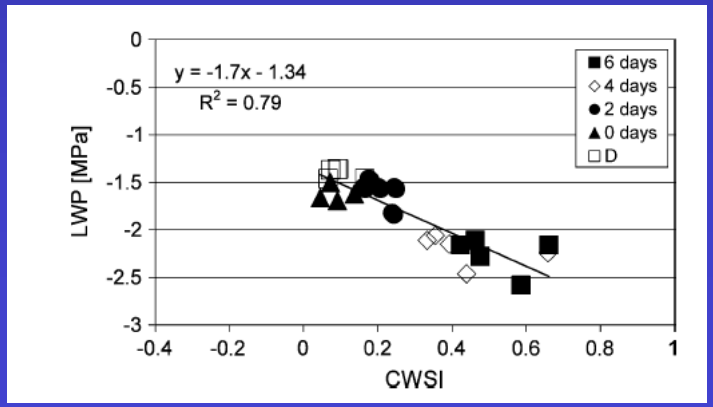

Journal of Experimental Botany, Vol. 56, No. 417, pp. 1843–1852, July 2005

Temperature distribution in canopy

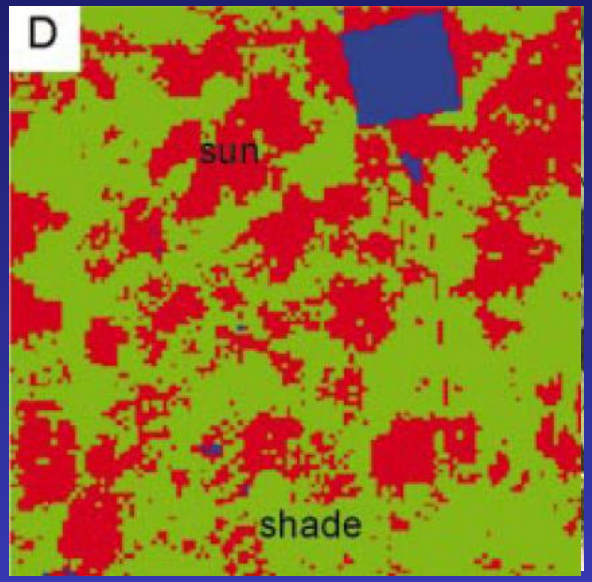

- Image processing requires overlying of thermal and visible image and subsequent classification of visible image
- Different distribution of temperature between sunlit and shaded leaves of *Vitis vinifera*
- Role of different irrigation (rainfall vs artificial watering)

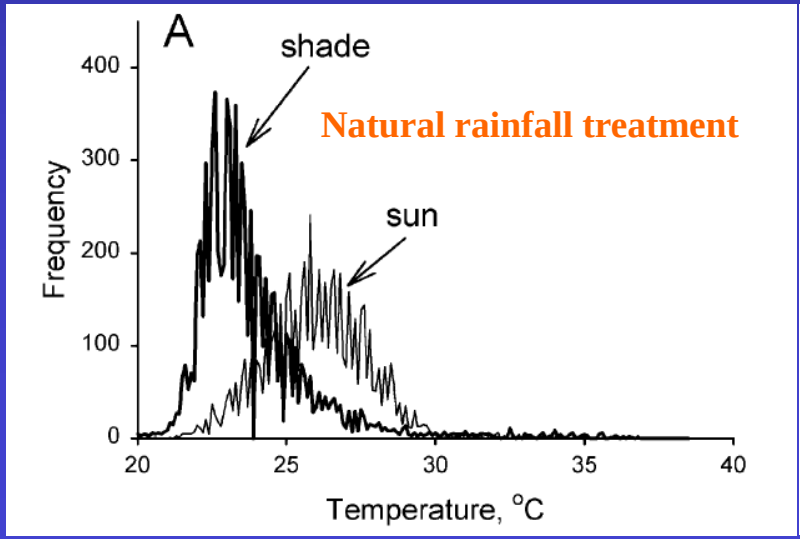

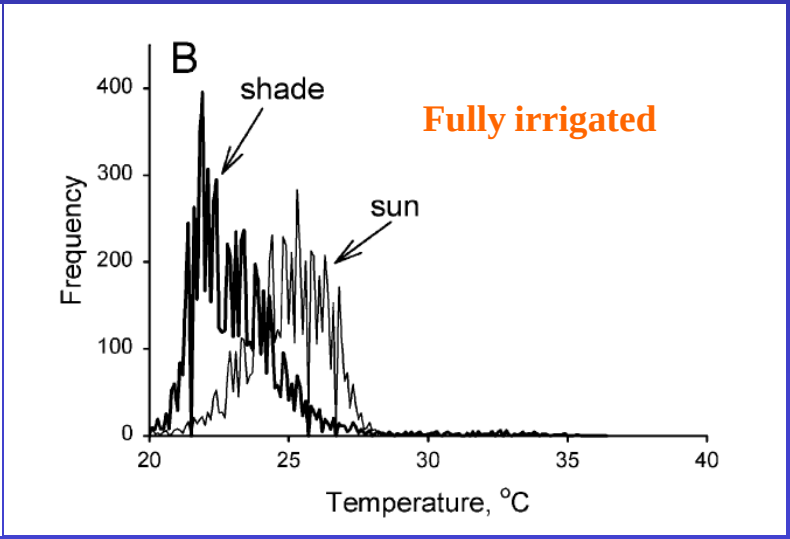

From: Leinonen and Jones 2006 JEB

Temperature distribution in canopy

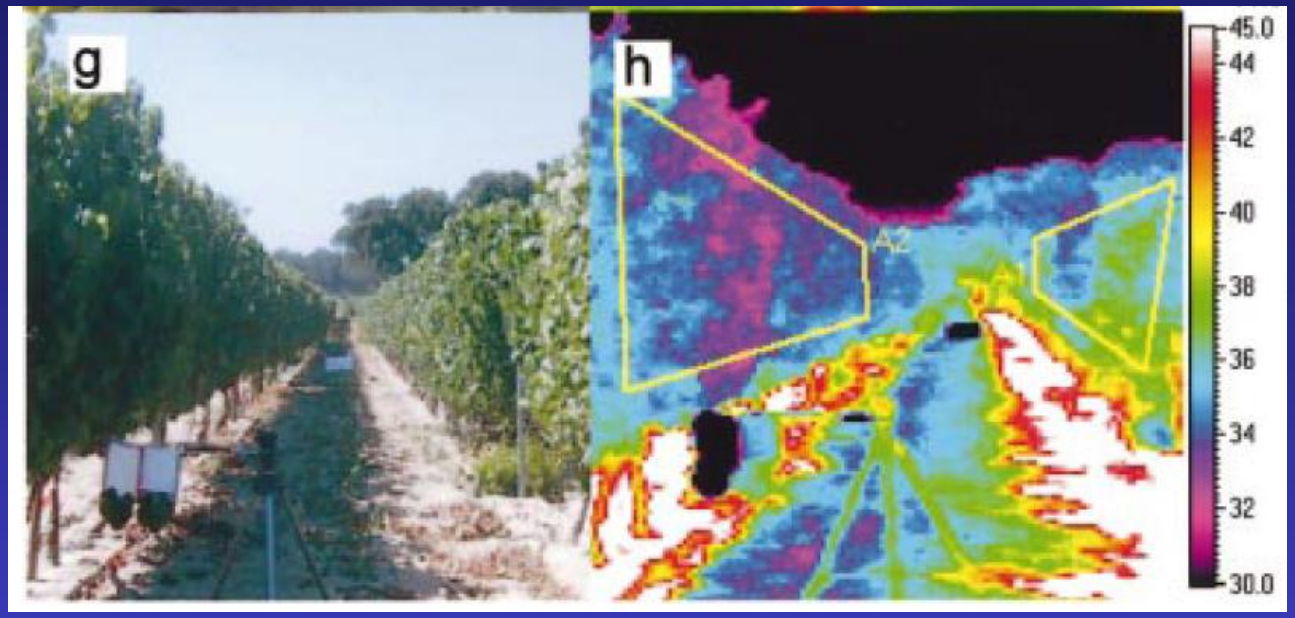

- Field thermoimaginery – combination of thermo and visible camera
- Different temperature distribution for sunlit and shaded leaves
- Shaded - lowered average temperature, broad temperature distribution

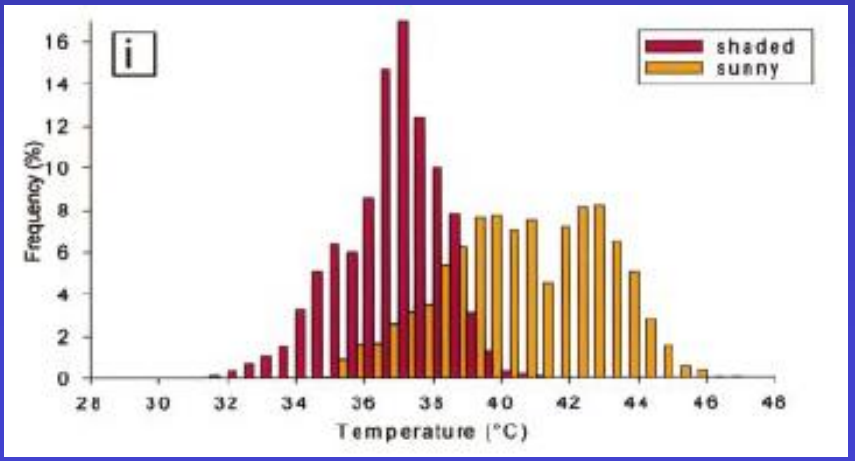

C. Biotic stress

Pre-symptomatic visualization of plant-virus interactions

- Salicylic acid produced as a signal in defense against pathogens close the stomata →temperature increase 8 hour before visible cells death

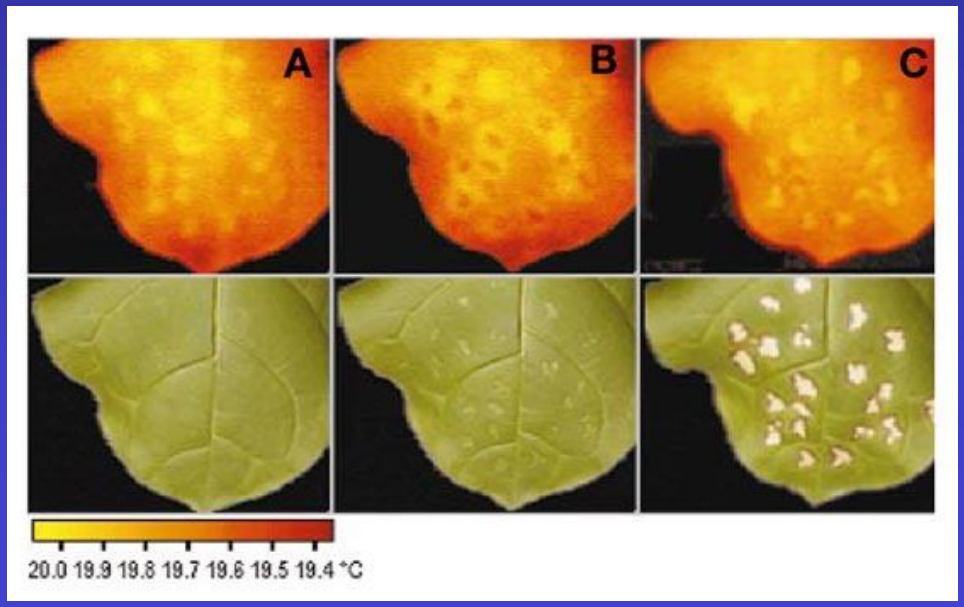

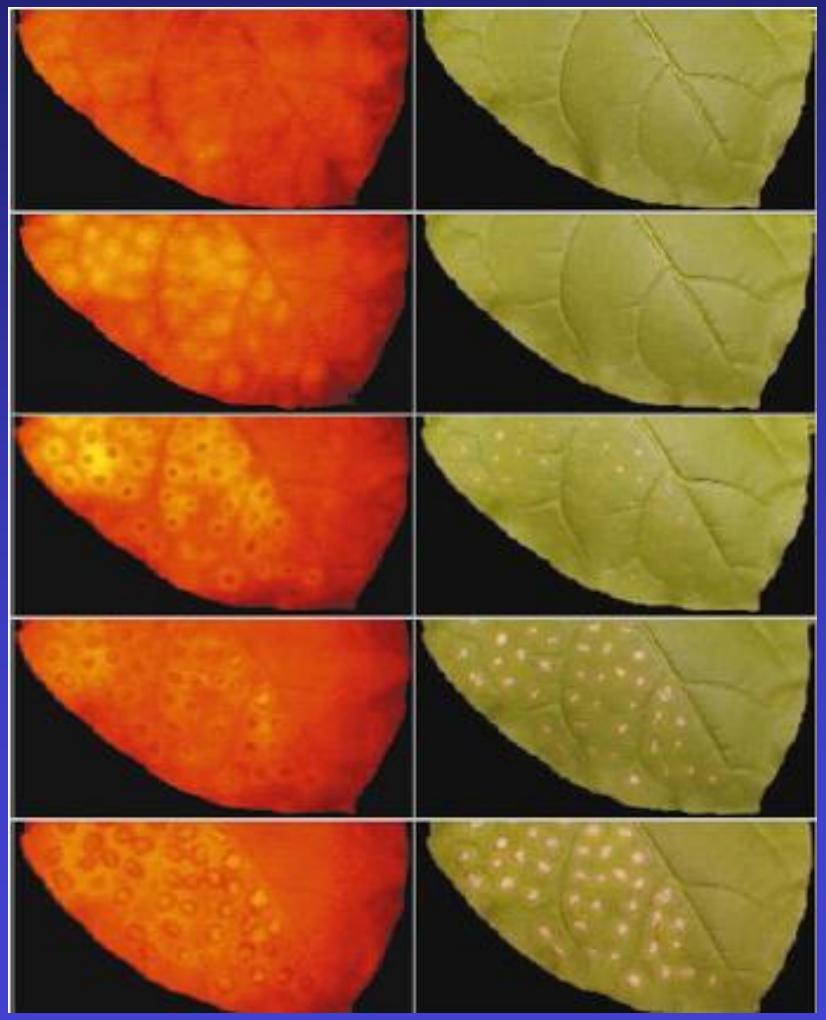

Chaerle L et al. 1998

E. PLANT THERMOGENESIS

- Thermogenesis in some special plant tissue in some species (spadix, flower, leaves etc.)
- Excess temperatures vary from few degrease up to 30°C (rapid incline – metabolic explosion)
- Role of alternative oxidase (cyanide independent oxidase) in heat production
- Protecting against cold nights, increase in odor of flowers etc.

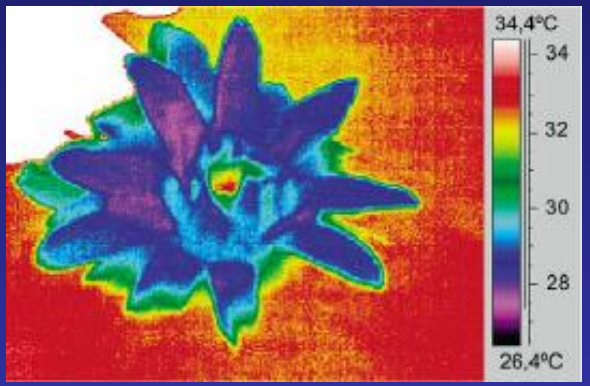

Thermogenesis in flowers of *V. Cruciana*

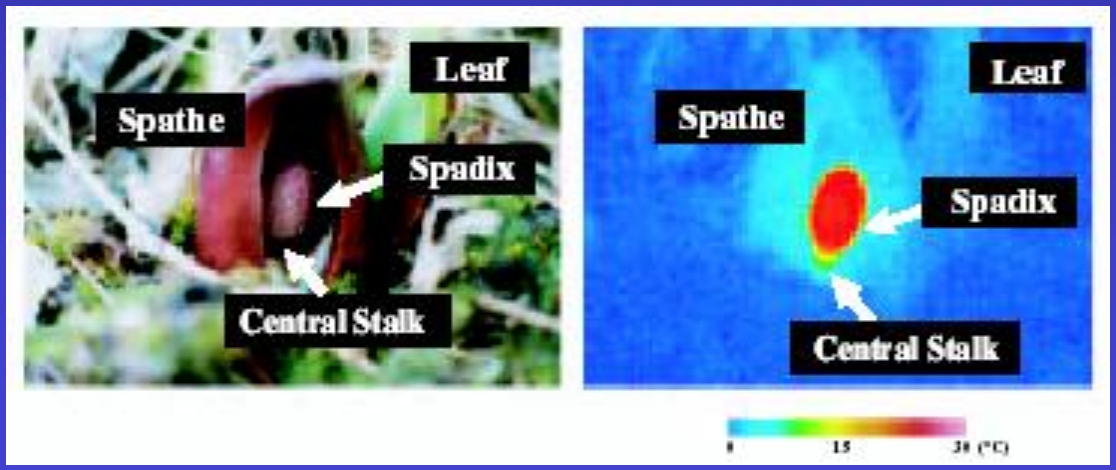

Thermogenesis in spadix of plant skunk cabbage at low temperature – maintaining of internal temperature around 20°C during reduction of ambient temperature below 0°C (Ito et al. 2003 PCE)

F. PHOTOSYNTHESIS RESEARCH

1. Relation between stomata conductance and primary or secondary photosynthetic reactions (Omasa 2003 PCP)
2. Leaf heating during stimulation of photoprotective non-photochemical quenching (Kaňa and Vass 2009 EEB)
3. Traspiration can reduce leaf temperature below critical levels – protection of photosynthesis (the heat most sensitive metabolic process)
4. Estimation of photosynthetic efficiency from energy balance

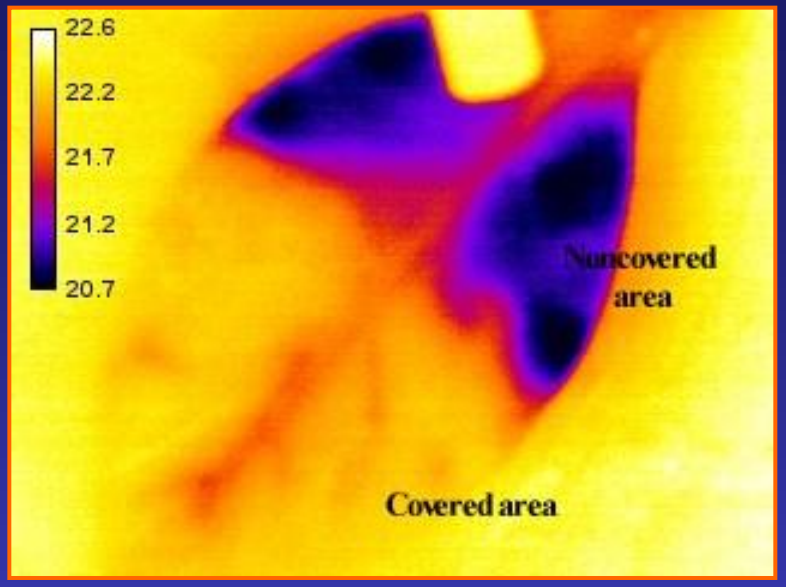

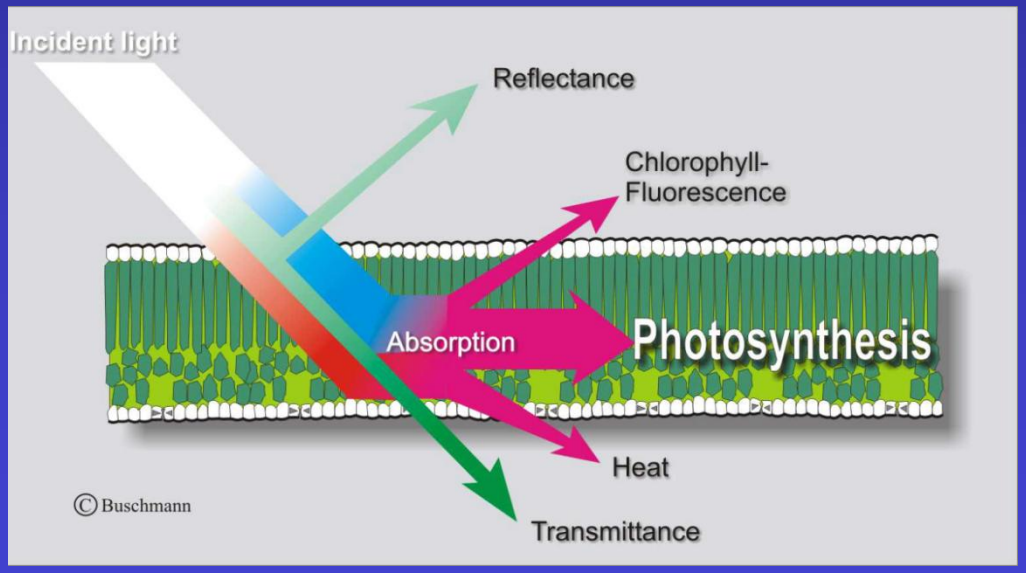

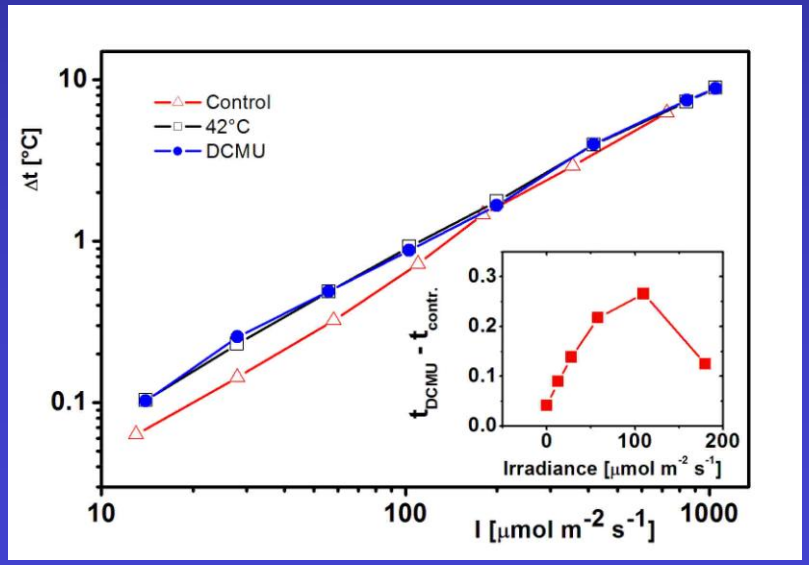

Stomatal conductance and Photosynthesis

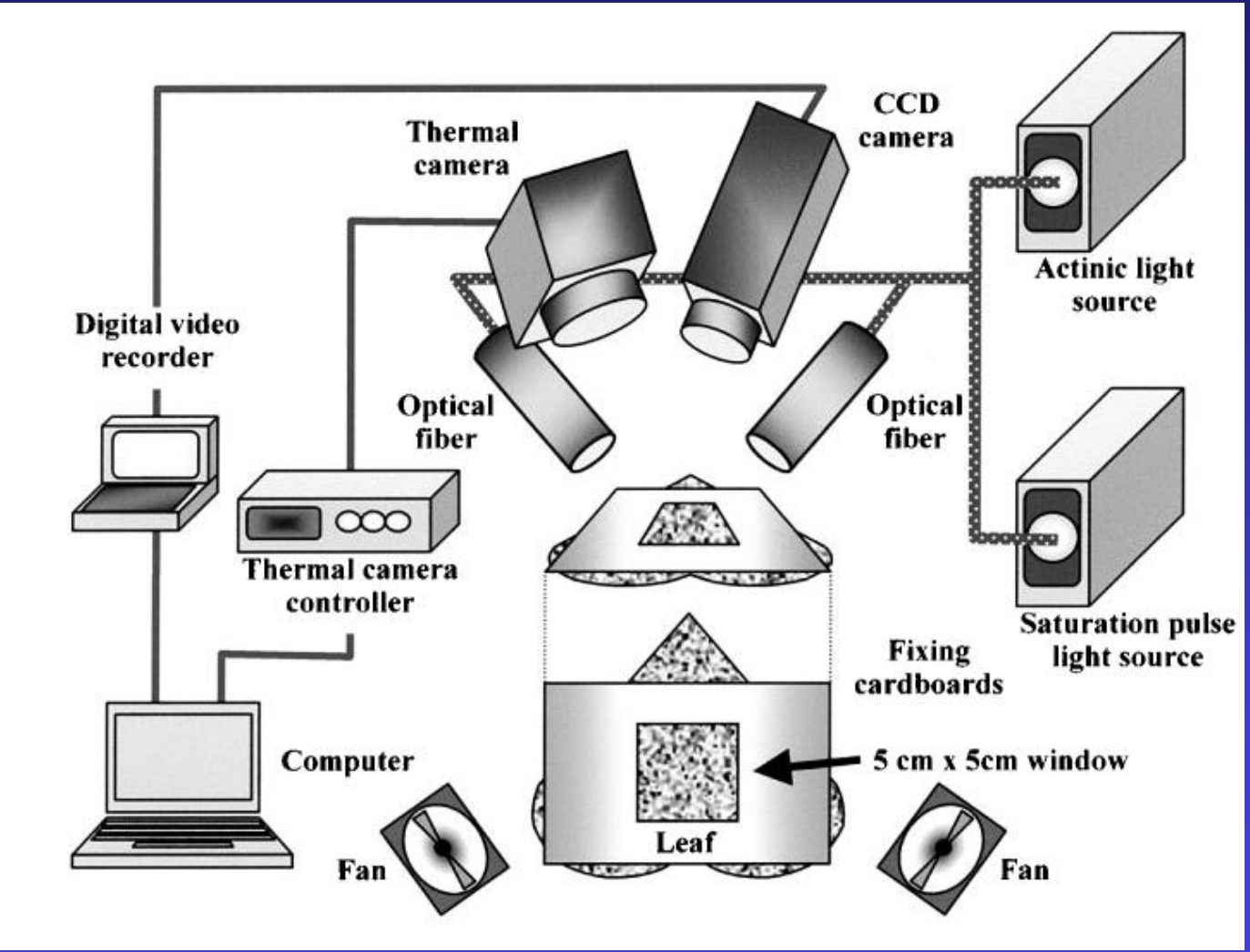

Omasa et al. 2003 PCP

STOMATAL CONDUCTANCE AND PHOTOSYNTHESIS

HIGH LIGHT

Independence of fluorescence and stomatal closure at high light

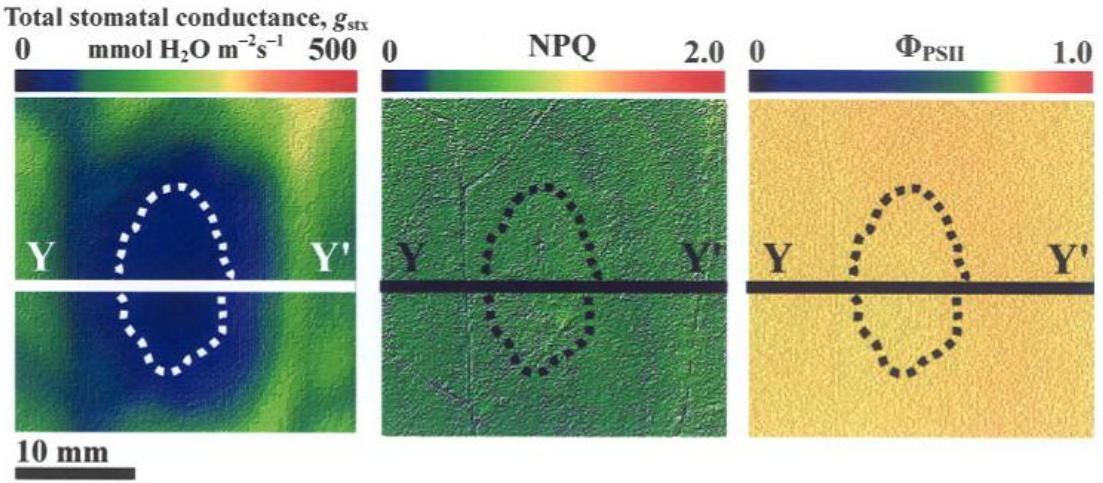

LOW LIGHT

fluorescence and stomatal closure correlation

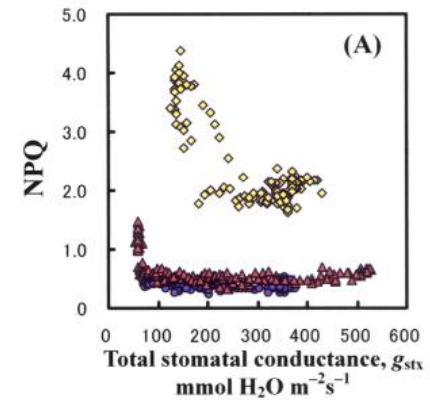

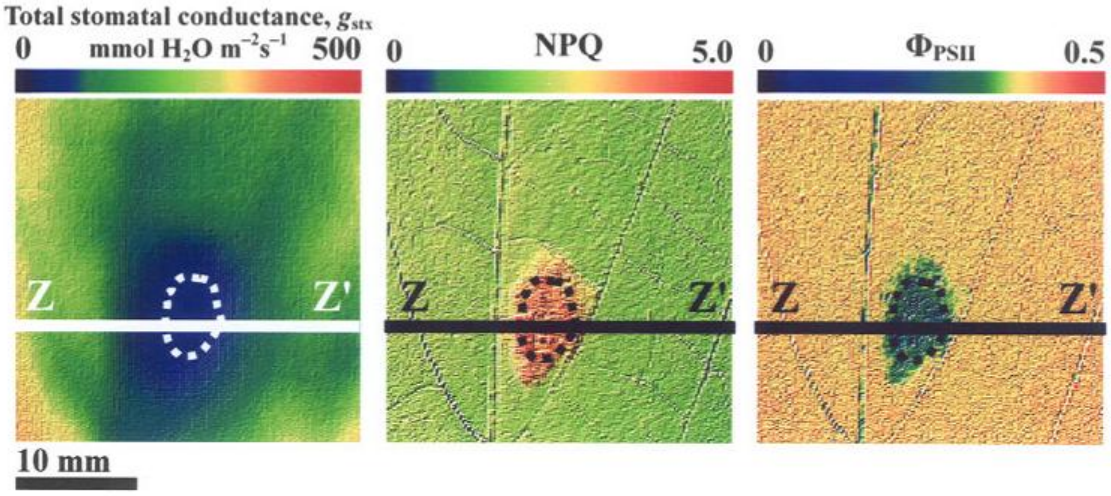

Omasa et al. 2003 PCP

Thermoimaging and NPQ

- Absorbed light can be utilized in photosynthesis (5-30%), emitted as fluorescence (8%) dissipate as a heat
- The extent of this dissipation is regulated by process called nonphotochemical quenching - NPQ
- NPQ can regulate light utilization in photosystem II - photoprotection against damage
- Complex process (dependent on PsbS protein, zeaxanthin formation, pH, antenna aggregation etc)

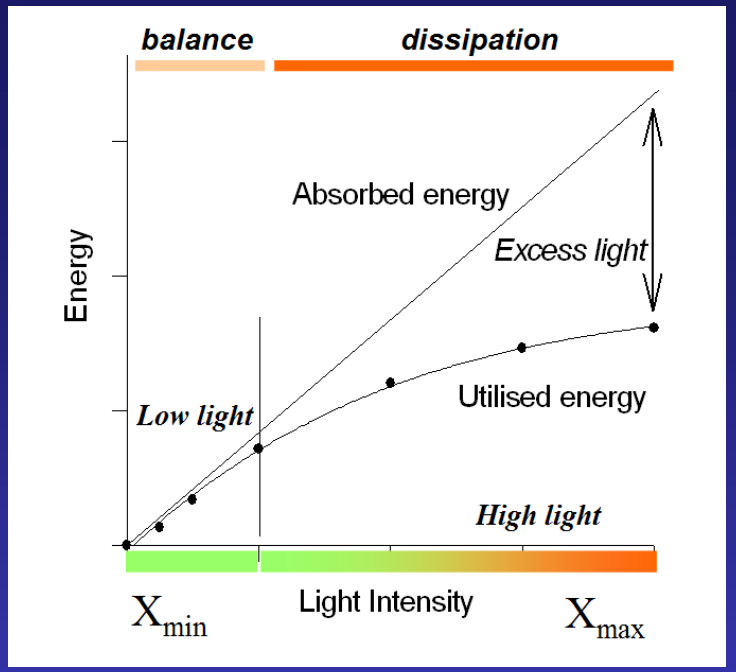

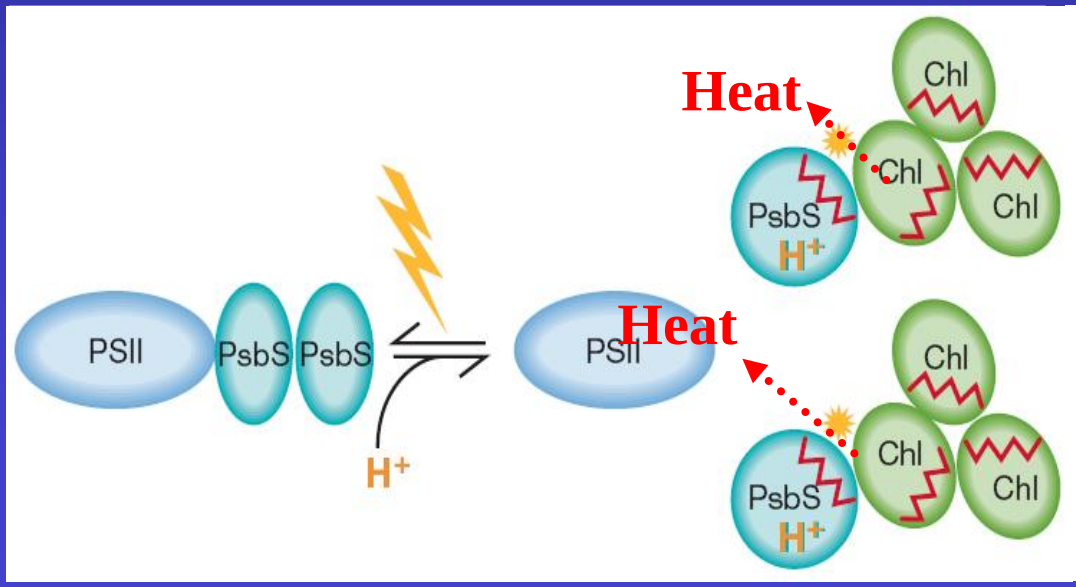

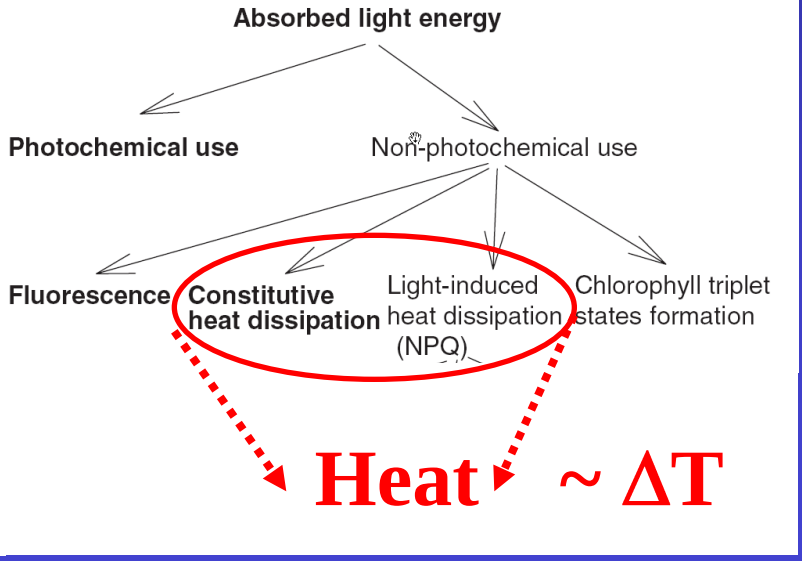

Experimental setup

- Thermocamera Varioscan 3200 ST (detection at 8-12μm, relative temperature resolution 0.03K, geometrical resolution 1.5 mrad, time response for picture 360x240 pixel, one picture every 1 sec), Fluorescence measurement (PAM 101/102)
- Role of transpiration in changes of temperature was checked by its elimination (by covering of leaf surface by vaseline jely)
- NPQ increase was induced by exposition to high irradiancy (up to 6 hours)

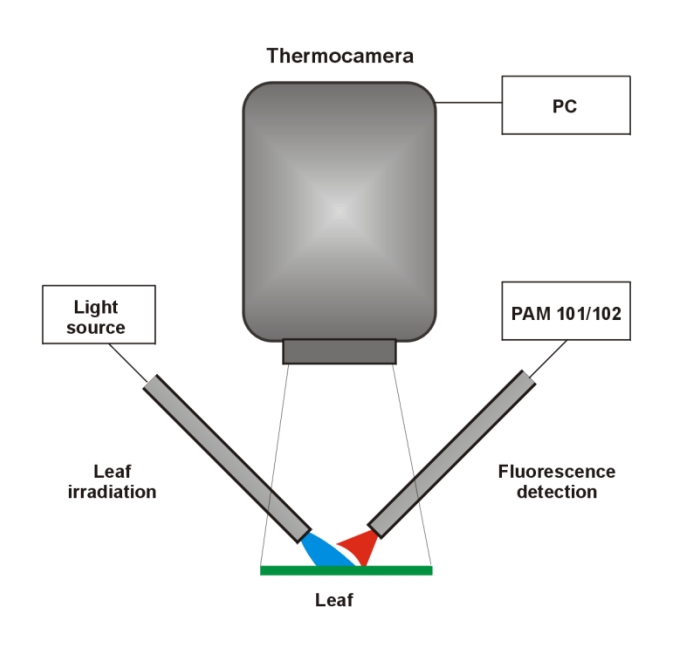

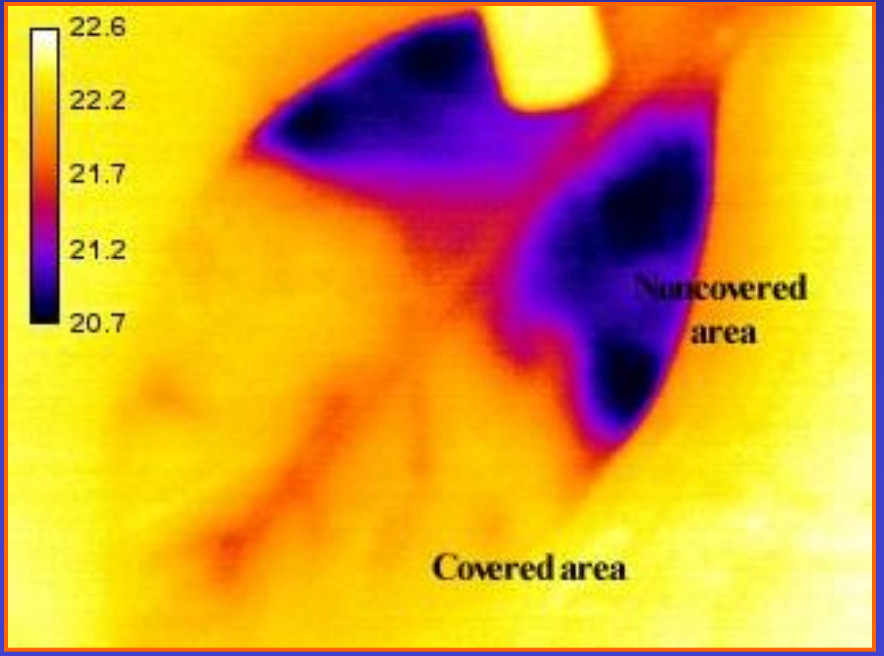

Elimination of transpiration

Vaseline jelly - elimination of evaporative cooling

⇩

homogenization of leaf surface temperature during heating

Homogeneity during irradiation

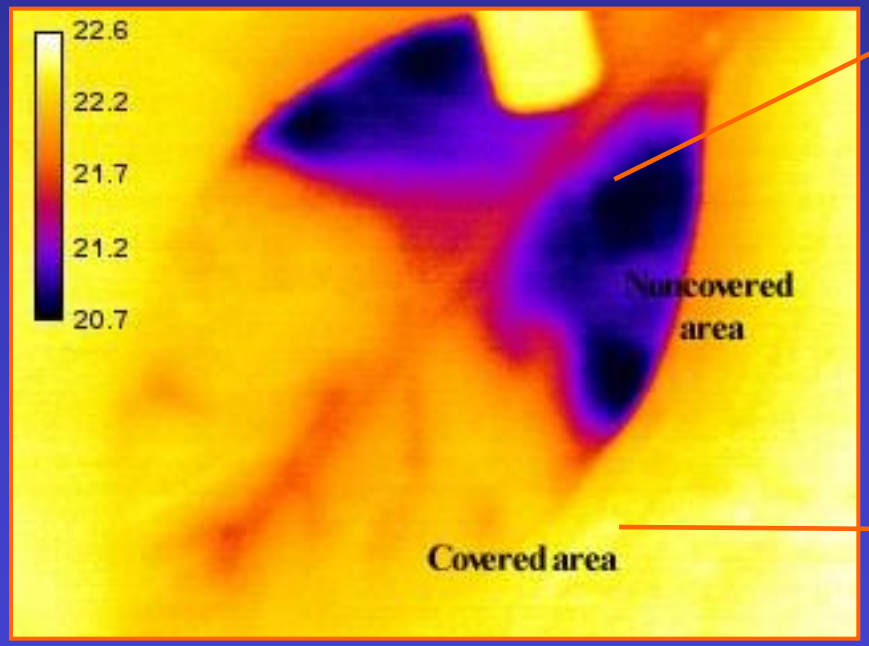

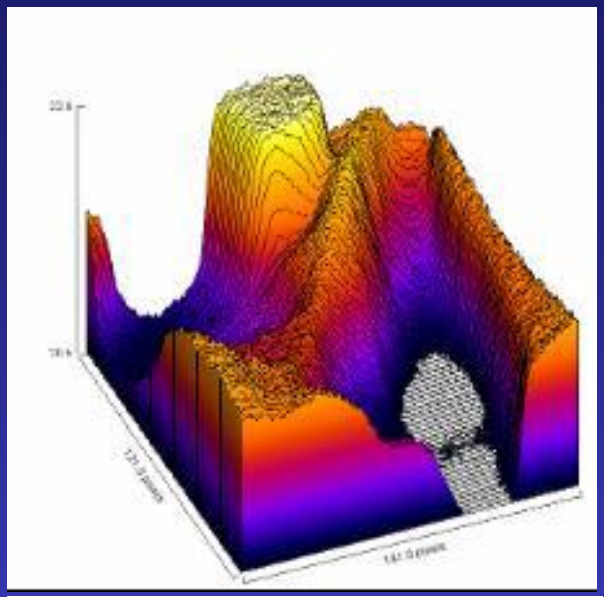

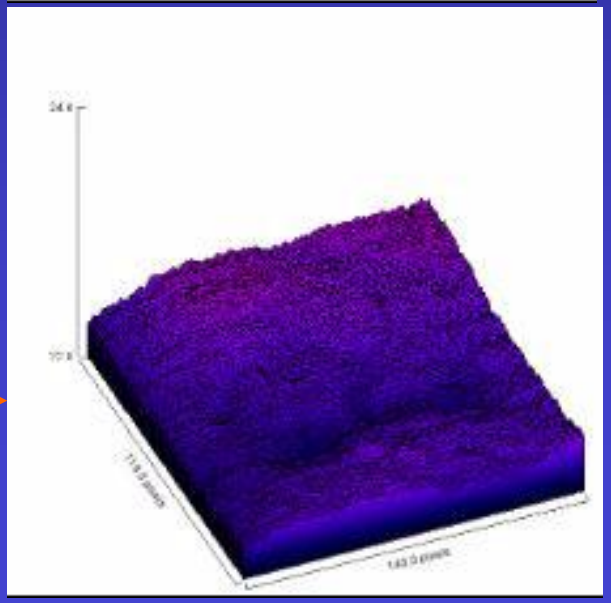

Changes in temperature during irradiation

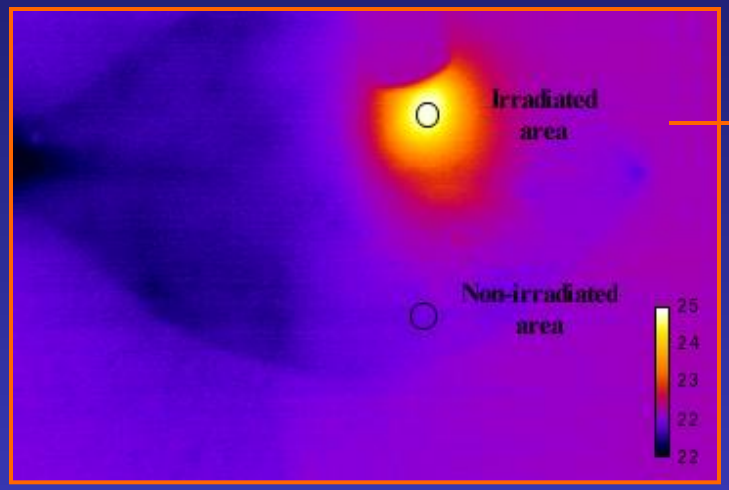

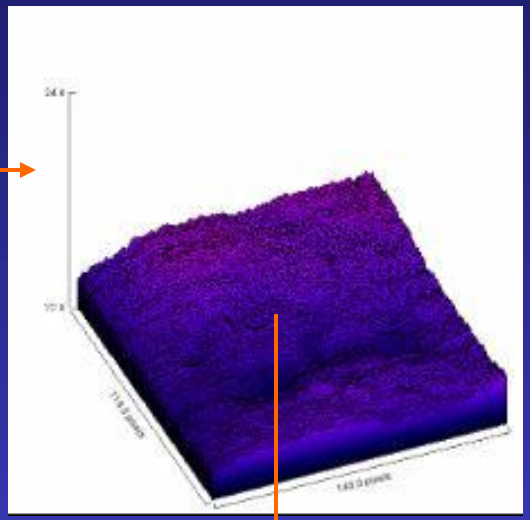

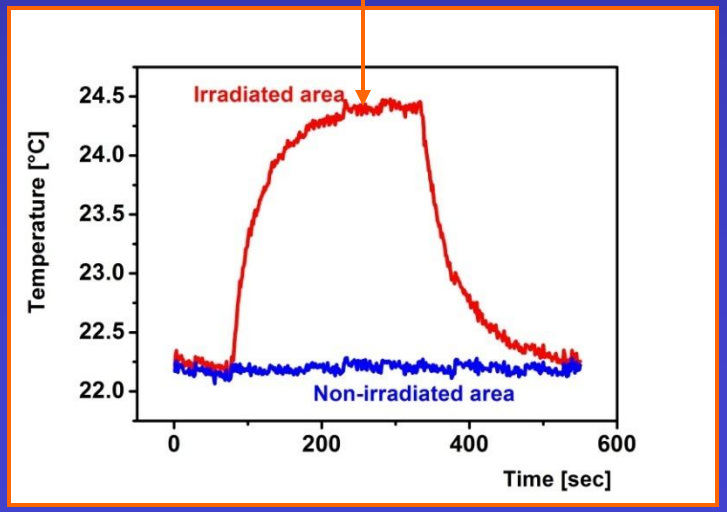

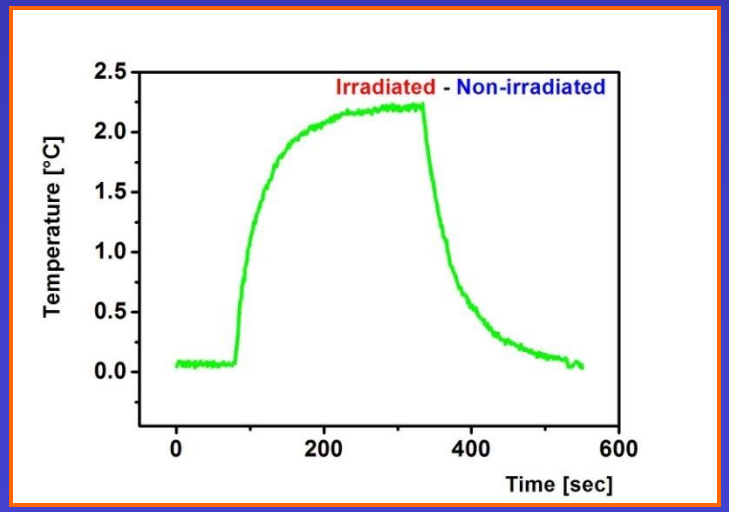

ENERGY DISSIPATION IN NON-PHOTOCHEMICAL QUENCHING

PHOTOSYSTEM II

HIGHER DISSIPATION BY NPQ IN „QUENCHED“ SAMPLE

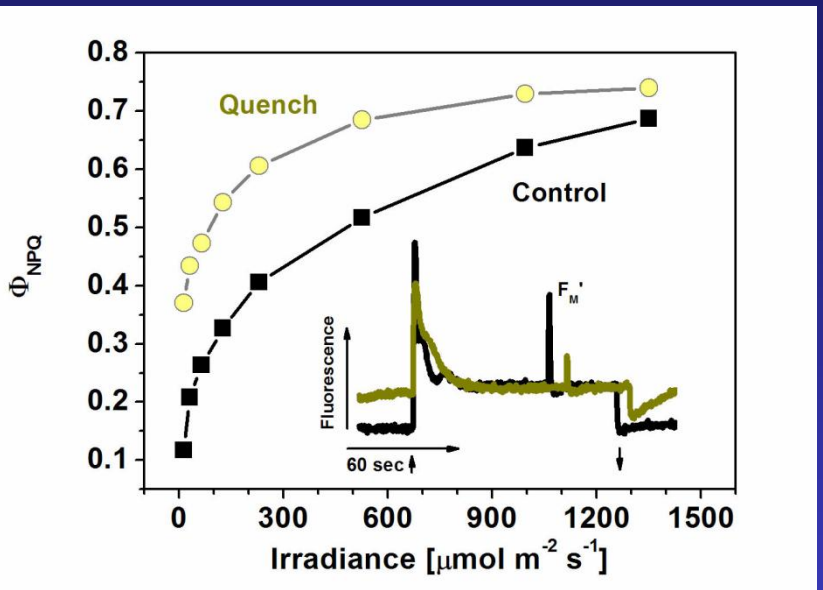

TEMPERATURE

HIGHER TEMPERATURE IN „QUENCHED“ SAMPLE

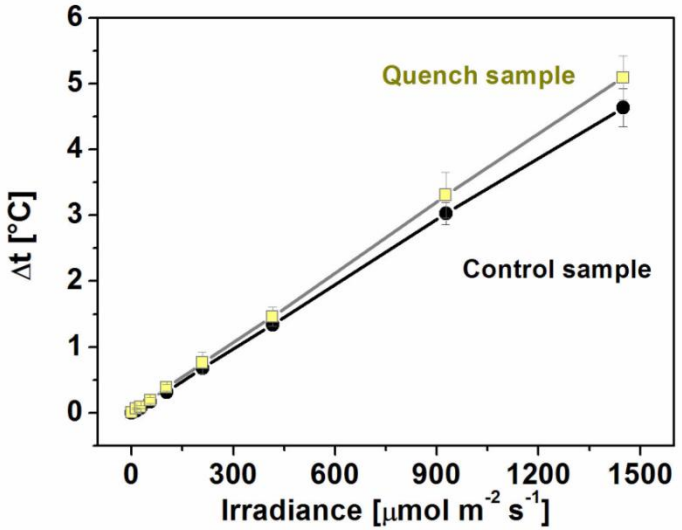

Kaňa a Vass 2009 EEB

MUTANT SELECTION

- Mutant selection (e.g. ABA insensitive mutant – *Merlot S et al . 2002 PJ*)
- ABA can trigger closure of stomata pores
- ABA insensitive mutants (*Abi1-1*) fails in stomata closure during draught stress – temperature decrease and water loss due to higher transpiration

Abi1-1 mutant

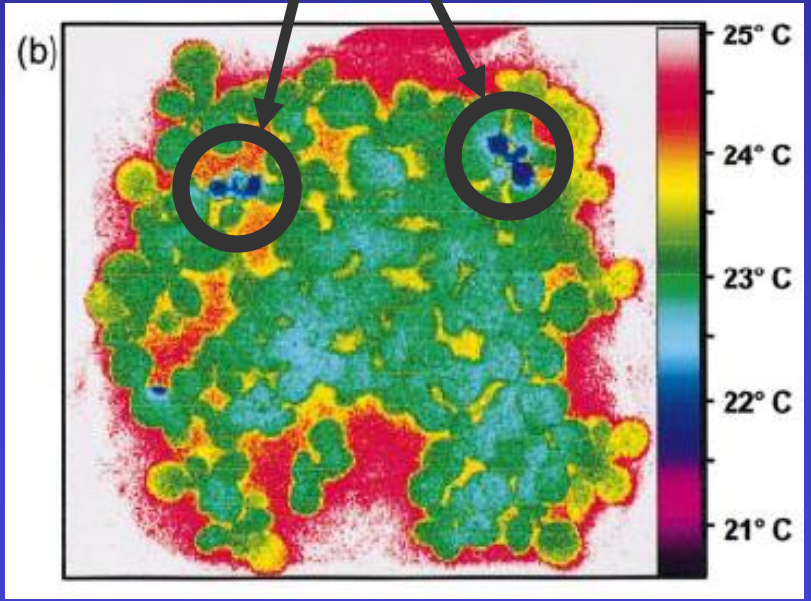

Plant phenotyping

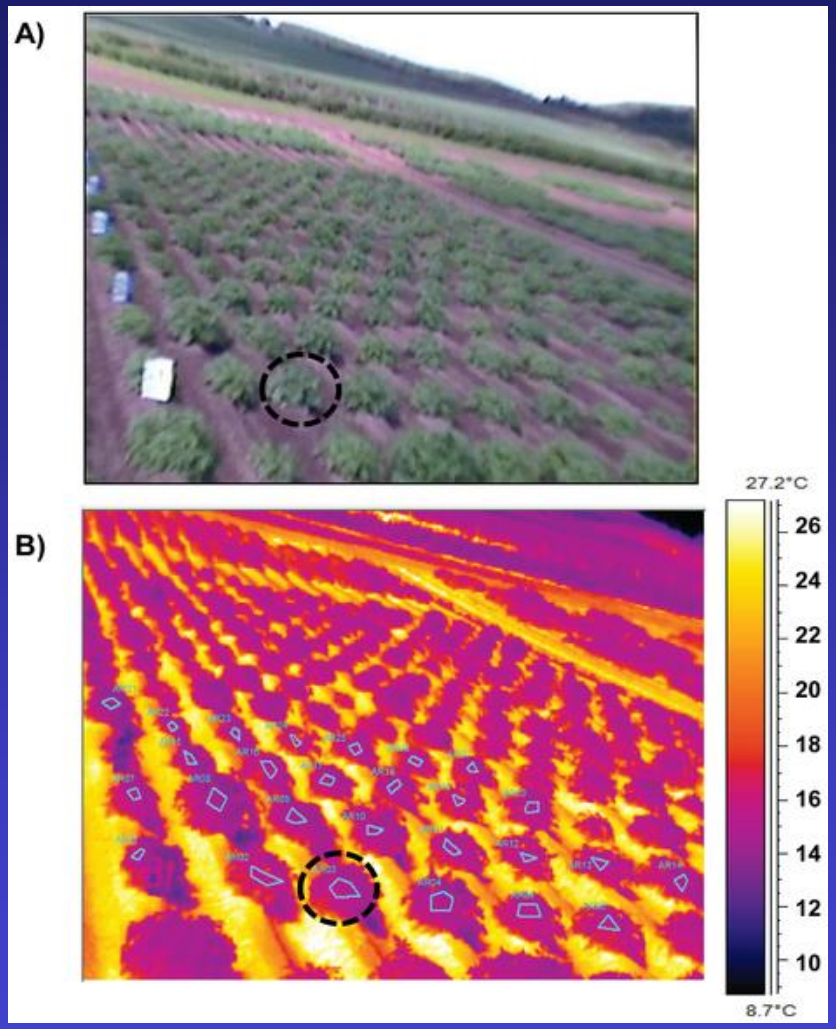

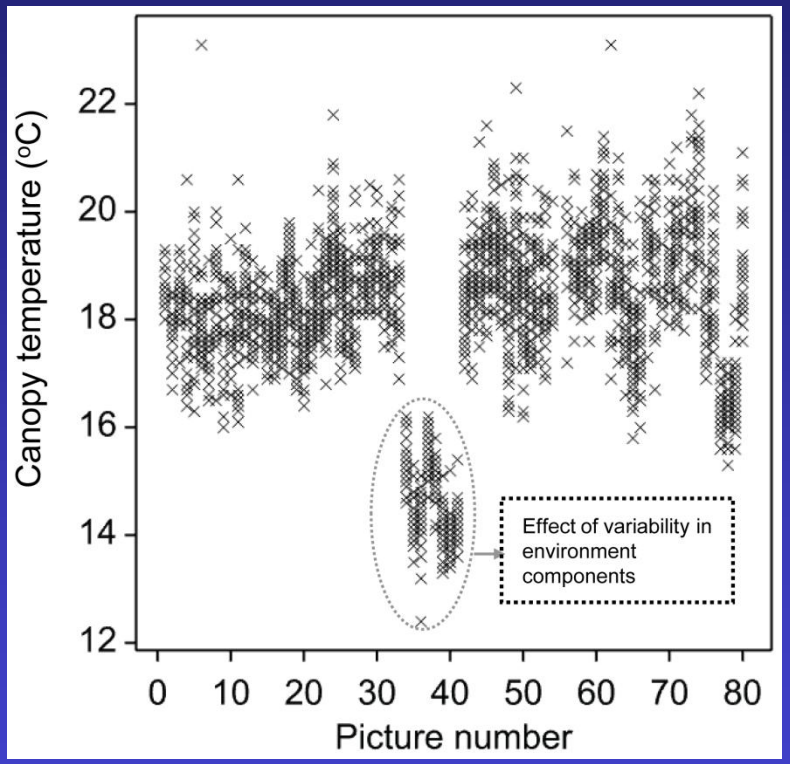

Prashar A, Yildiz J, McNicol JW, Bryan GJ, et al. (2013) Infra-red Thermography for High Throughput Field Phenotyping in Solanum tuberosum. PLoS ONE 8(6): e65816. doi:10.1371/journal.pone.0065816
http://www.plosone.org/article/info:doi/10.1371/journal.pone.0065816

PLOS | ONE

THANK FOR YOUR ATTENTION

Environmental and Experimental Botany 64 (2008) 90–96

Contents lists available at ScienceDirect

Environmental and Experimental Botany

journal homepage: www.elsevier.com/locate/envexpbot

Thermoimaging as a tool for studying light-induced heating of leaves Correlation of heat dissipation with the efficiency of photosystem II photochemistry and non-photochemical quenching

Radek Kaňa[a,b,c,*], Imre Vass[a]

[a] Biological Research Center, Institute of Plant Biology, Szeged H-6701, Hungary
[b] Institute of Microbiology, Academy of Sciences of the Czech Republic, Opatovický mlýn, 379 81 Třeboň, Czech Republic
[c] Palacký University, Faculty of Science, Laboratory of Biophysics, tř. Svobody 26, 771 46 Olomouc, Czech Republic

ARTICLE INFO

Article history:
Received 28 June 2007
Received in revised form 31 January 2008
Accepted 24 February 2008

Keywords:
Thermoimaging
NPQ
Photosystem II efficiency
Leaf temperature
Energy balance equation of leaf

ABSTRACT

Thermoimaging – a highly sensitive and non-invasive method of temperature measurement – was applied to explore the role of changing photosynthetic efficiency in light-induced heating of tobacco (*Nicotiana tabacum cv. Samsun*) leaves. In the absence of evaporative cooling through the stomata, which was achieved by covering leaves with Vaseline, illumination with 50–1400 μM photons m^{-2} s^{-1} intensity of photosynthetically active radiation resulted in ≈1–5 °C leaf temperature increase in about 2 min. The heating effect showed a non-linear correlation with the extent of non-photochemical quenching (NPQ) resulting in higher leaf temperatures at higher NPQ values. When leaves were adapted to excessive irradiance (1300 μM photons m^{-2} s^{-1} for 6 h), which resulted in reduction of photosynthetic efficiency and amplification of NPQ the light-induced heating effect was enhanced. The experimental results have been explained on the basis of a simple theoretical model characterizing the balance of energy fluxes in leaves in relation to the efficiency of photosystem II photochemistry and non-photochemical quenching. The role of alternative energy dissipation pathways outside of PSII in the phenomenon of light-induced leaf heating is also discussed.

1. Introduction

Thermoimaging is a non-destructive method suitable for monitoring spatial distribution of temperature over the leaf surface based on non-contact infrared radiation measurement (Jones et al., 2003). All applications of infrared thermography in plant biology utilize some aspects of the energy balance equation of plants, i.e. the energy conservation law. It declares that the sum of heat content in the leaf tissue reflected in its temperature is constant (see, e.g. Jones, 2004a for review). Internal metabolic processes in plant tissues or absorption of radiation can increase this heat content, and on the contrary water evaporation, heat convection and heat conduction are able to reduce it. Therefore, thermoimaging has already been applied for the detection of thermogenesis in plant tissues (see, e.g. Lamprecht et al., 2002), measurement of stromata conductance (Jones et al., 2002, Leinonen et al., 2006), detection of water stress (see, e.g. Jones et al., 2002; Jones, 2004b; Cohen et al., 2005), or detection of other stresses such as virus infection (see Chaerle et al., 2004) or mutations (see, e.g. Merlot et al., 2002) resulting in reduction of water content or stomata conductance.

So far, only few works have dealt with the application of temperature detection by thermoimaging in photosynthesis research even though photosynthesis can store more than 30% of incident irradiance (Delosme, 2003). Photothermal radiometry measurements by infrared detector (see details on methods in Nordal and Kanstad, 1981) have shown the applicability of this method in

Abbreviations: ABA, absicic acid; Chl a, chlorophyll a; C, vertical energy heat flux from the irradiated leaf spot to the surrounding air; F_0 (F_M), the minimal (maximal) chlorophyll a fluorescence for dark adapted state; F_m', maximal fluorescence of light adapted leaves; F_S, steady state Chl a fluorescence of light adapted leaves; $\Delta\Phi_H$, difference in the quantum efficiency of photosystem II photochemistry between control and quenched samples; Φ_H, quantum efficiency of photosystem II photochemistry; Φ_D, overall efficiency of light energy dissipation into heat; Φ_{NO}, efficiency of a non-light-induced (basal or dark) quenching process; Φ_{NPQ}, efficiency of light dissipation by non-photochemical quenching; g_B (g_L), boundary (leaf) conductance for heat; *I*, intensity of incident flux of light; NPQ, non-photochemical quenching; P, energy flux into photosynthesis; PSII, photosystem II; ΔT, temperature difference between the irradiated and dark part of leaf.

* Corresponding author at: Institute of Microbiology, Academy of Sciences of the Czech Republic, Opatovický mlýn, 379 81 Třeboň, Czech Republic.
Fax: +420 38434041.
E-mail address: kana@alga.cz (R. Kaňa).

0098-8472/$ – see front matter © 2008 Elsevier B.V. All rights reserved.
doi:10.1016/j.envexpbot.2008.02.006

photosynthesis research in general (Bults et al., 1982, Malkin et al., 1991, Driesenaar et al., 1994), which showed similar efficiency of photosynthesis as obtained from photoacoustic measurements (Kanstad et al., 1983). However, similar results have not been obtained with thermal imaging that can scan variations of temperature over the whole leaf surface. Only some recent works (see, e.g. Omasa and Takayama, 2003 and West et al., 2005) used thermal imaging for correlation of stomata conductance calculated from temperature changes with measurement of photosynthetic efficiency from Chl a fluorescence (see, e.g Maxwell and Johnson, 2000 for review). In these works, ABA treatment (Omasa and Takayama, 2003) or reduced CO_2 content (West et al., 2005) was accompanied by temperature changes due to stomata closure or opening that was accompanied by changes of PSII photochemistry together with the efficiency of light utilization as characterized by non-photochemical quenching (NPQ) (Omasa and Takayama, 2003). NPQ is an important mechanism for regulating the fate of absorbed energy in photosynthetic organisms for utilization in photosynthesis and dissipation to heat (Horton and Ruban, 2005). The molecular mechanism of NPQ is very complex and include many specific processes such as lumen acidification, zeaxanthin formation in the xanthophyl cycle or triggering by the PsbS protein (see, e.g. Horton et al., 2005). All these effects together result in lower efficiency of PSII photochemistry and increased heat dissipation when high NPQ is developed.

Here, we used thermal imaging for direct and very accurate measurement of temperature over the leaf surface in parallel with variable Chl a fluorescence to detect photosynthetic activity under various irradiation conditions. Such simultaneous measurements of temperature and fluorescence allowed us, for the first time, to detect leaf temperature increase at different values of NPQ. This experimentally measured correlation of light energy dissipation and the increase in leaf temperature has been simulated by a simple theoretical model, which takes into account the energy balance of leaf and ascribes the NPQ dependent temperature changes to the reduction in the efficiency of PSII photochemistry.

2. Materials and methods

2.1. Plant material and light treatment

The experiments have been carried out with fully developed detached leaves of 4 months old tobacco plants (*Nicotiana tabacum cv. Samsun*), which were cultivated in greenhouse with controlled temperature of 25 °C, and irradiancy of about 200 μM photons m^{-2} s^{-1} of PAR. Adaptation to high light was induced by 6 h irradiation (1300 μM photons m^{-2} s^{-1}) provided by a cold-light halogen lamp KL 1500 Electronic (Schott AG, Mainz, Germany).

2.2. Temperature measurements by thermal imaging, data acquisition and analysis

The temperature of leaf surface was determined with a Varioscan 3200 ST (Jenoptik, Germany) sterling-cooled infrared scanning camera that detects temperature with relative resolution of 0.03 K based on measurement of infrared radiation at 8–12 μm. The camera has geometrical resolution of 1.5 mrad with 30° × 20° maximal field of view lens, and operates on the principle of object scanning that gives spatial resolution of 360 × 240 pixels. The pictures were captured with maximal frequency of image refreshing (1 Hz) and the electro-optical zoom was used to reduce the angle of camera aperture to 21° × 14°. This set-up led to spatial resolution of camera of about 0.22 mm per pixel for focus distance 0.3 m (see, e.g. Jones, 2004a).

The ambient radiation reflected by the leaf surface and radiation of the air path between the leaf and the camera was subtracted by the camera software during recalculation of radiation to temperature. The background temperature necessary for this subtraction was determined as the temperature of a mirror in a similar position as the leaves of interest. The temperature of air path between the leaf and the camera was measured by thermometer and the emissivity was set at 0.95 reflecting its typical value for leaves (see review by Jones, 2004a).

Light-induced changes in the leaf temperature have been induced by irradiation of an 8 mm spot of the leaf by blue light, which was provided by a halogen lamp (KL 1500 Electronic; Schott AG, Mainz, Germany) equipped with light guide and blue broad bandpass filter. The lamp has efficient heat filtering to avoid direct heating of leaves by infrared radiation. The irradiated spot of the leaf was exposed at a given irradiancy for 2–3 min to reach steady-state value of temperature. To saturate photosynthesis a flash of PAR (6000 μM photons of m^{-2} s^{-1} intensity for 800 ms) was applied.

Covering of leaf surface by Vaseline jelly before measurement eliminated evaporative cooling (see, e.g. Leinonen et al., 2006). The heating of leaf has been calculated as difference between the irradiated spot and the non-irradiated part on the same leaf for all used irradiancies. Recorded images were analyzed by public domain Java image processing program ImageJ 1.32b (see, e.g. Abramoff et al., 2004 and Rasband, 1997–2008) and presented in false colors. The pictures were imported into the ImageJ software and the values of light-induced temperature changes have been calculated as the average values of a small circular area (10 pixels) in the middle of the irradiated spot.

2.3. Fluorescence measurements

The fluorescence measurements have been carried out with a PAM 101/102 fluorometer (Walz, Germany). Before experiments, the light guide of PAM was aligned to about 5 mm far from the leaf surface in a way not to shadow the measured area. This set-up allowed simultaneous fluorescence and temperature measurement.

The parameters characterizing the efficiency of light utilization in PSII in photochemical (Φ_{II}) and non-photochemical way (Φ_{NPQ} and Φ_{NO}) were calculated according to Kramer et al. (2004). Φ_{II} represents the quantum efficiency of PS II (Genty et al., 1989), Φ_{NPQ} is the yield of light dissipation by down regulation due to NPQ, and Φ_{NO} is defined as a yield of non-light-induced (basal or dark) quenching process (see Kramer et al., 2004 for details). The minimal (F_0) and maximal (F_M) Chl a fluorescence of dark adapted samples (necessary for Φ_{II}, Φ_{NPQ} and Φ_{NO} calculations) were obtained before or during application of a saturating flash of PAR (with 6000 μM photons m^{-2} s^{-1} intensity and 800 ms duration) for dark adapted leaves. Steady state Chl a fluorescence of light adapted leaves (F_S, F_0' and F_M') was measured after 2 min at the given irradiancy just before application of the saturating flash (F_S), or at the maximum of saturating flash (F_M'). F_0' was measured after termination of actinic light and application of far red light for 2 s.

2.4. Theoretical model of light utilization

The energy balance for a leaf is defined by the following equation:

$$R_n + M - \lambda E - C = \rho_{leaf} c_p l_{leaf} \frac{dT_{leaf}}{dt} = S \quad (1)$$

where R_n is the net radiant flux density absorbed (see, e.g. Jones, 2004a), M is the rate of heat produced by metabolism, λE is the rate of heat loss through evaporation of water (transpiration), C is the rate of heat loss by conduction or convection to the environment, S is the rate of increase of the heat content of leaf tissue where ρ_{leaf} is its density, c_p specific heat of leaf, l_{leaf} thickness and T_{leaf} is temperature. For further theoretical calculation, energy losses due to infrared radiation emitted at room temperature have been neglected. Thus R_n including emitted infrared radiation (see, e.g. Jones, 2004a) has been replaced by the incident irradiancy (I) in Eq. (1). In the case of eliminated evaporation ($E = 0$), and assuming that the whole metabolic energy flux goes into photosynthesis ($M = -P$, where P is the energy flux to photosynthesis), the steady state energy balance can be rewritten as

$$I - P - C = 0 \tag{2}$$

Eq. (2) further assumes that the heat content is not changing as a function of time as thermal equilibrium has been already reached. For further quantitative parameterization of the model, we assumed two vertical heat fluxes C: (1) vertical heat flux from the irradiated leaf surface to the surrounding boundary air layer above the irradiated leaf surface; (2) vertical heat flux from the irradiated leaf surface to the leaf tissue below the irradiated spot. Other possible pathways of energy fluxes (e.g. lateral heat conduction) have been neglected as we have characterized energy loss by conduction only qualitatively because it is expressed only in the constant K (see Eq. (6)) that is dependent only on the physical parameters but it is same for control and quenched leaf. Moreover, most of the incident light is absorbed inside the upper thin layer of leaf (90% in the layer of 0.1 mm) (see Cui et al., 1991). Therefore heat transfer proceeds mostly vertically from this small upper layer of leaf because its diameter is several times bigger (it was about 10 mm) than this layer.

The boundary layer of a leaf is a thin layer of air above the leaf surface (see, e.g. Schuepp, 1993) whose heat conductance is dependent on several factors such as leaf shape and surface, and velocity of air above the leaf, (see, e.g. Cambell and Norman, 1998). As all these physical and aerodynamic parameters of the leaf and the leaf boundary air layer were kept constant during the measurements, we have assumed constant heat flux through the boundary air layer. In conclusion, the energy flux represented by C in Eq. (2) is dependent on the temperature difference between the irradiated spot and ambient temperature, and on the sum of boundary and leaf conductance. Thus, C can be expressed as

$$C = (g_B + g_L)(T_{leaf} - T_a) \tag{3}$$

where g_B and g_L are boundary and leaf conductance for heat, T_{leaf} and T_a are the measured temperature of the irradiated leaf surface and the surrounding ambient air. We defined the efficiency of utilization of incident irradiation (I) in photosystem II (Φ_{II}) and light energy that is dissipated in heat (Φ_D) as follows

$$\Phi_{II} = \frac{P}{I} \tag{4}$$

$$\Phi_D = \frac{D}{I} \tag{5}$$

where D is the energy that was not used in photosynthesis and wasted as heat, P is the energy flux into photosynthesis. Φ_D is considered to be a theoretical analog of the sum of Φ_{NPQ} and Φ_{NO} measured from Chl a fluorescence. Taken Eqs. (2)–(5) together $\Delta T = T_{leaf} - T_a$ can be expressed as

$$\Delta T = \frac{I(1 - \Phi_{II})}{K} \tag{6}$$

where K is defined as the sum of g_B and g_L. The g_B and g_L values are assumed to be dependent on the air (k_A) and leaf (k_L) conductivity, and on the thickness of leaf (d_L) and surrounding boundary layer (d_B) according to the equations:

$$g_B = \frac{k_A}{d_B} \tag{7}$$

$$g_B = \frac{k_L}{d_L} \tag{8}$$

The values of k_A and k_L have been obtained from literature as 0.026 and 0.2 W m^{-2} K^{-1}, respectively (see, e.g. Jones, 1992), and d_L and d_B has been kept constant for simplicity of model parameterization ($d_L = 3\ 10^{-3}$ m and $d_B = 1\ 10^{-3}$ m). According to the previous equations and parameters, the value of parameter K has been calculated as 55 W m^{-2} K^{-1}.

The experimentally determined dependence of Φ_{II} on light intensity has been approximated by curve fitting using the $\Phi_{II} = A_1 \exp(-I/t_1) + y_0$ function in the 0–1400 μM photons m^{-2} s^{-1} range. The obtained $\Phi_{II}(I)$ values have been then used for calculation of ΔT in Eq. (6), and of Φ_D in Eq. (9):

$$\Phi_D = 1 - \Phi_{II} \tag{9}$$

The light intensity dependence of the difference between calculated values of Φ_{II} for control and quenched leaves ($\Delta\Phi_{II}$) can be written as

$$\Delta\Phi_{II} = K\frac{(\Delta T_{quench} - \Delta T_{control})}{I} \tag{10}$$

where $\Delta T_{control}$ and ΔT_{quench} are the values calculated from Eq. (6) using Φ_{II} for control and quenched leaves respectively.

3. Results and discussion

The main aim of our research was to explore the role of reduced efficiency of photosynthesis on light-induced heating of leaves. Leaf temperature changes were measured on detached tobacco leaves covered by Vaseline in order to exclude the effect of evaporation. A typical thermoimage of a leaf half covered with Vaseline is shown in Fig. 1. The Vaseline layer eliminates evaporative cooling of the leaf that can decrease the leaf temperature by about 2° below the temperature of the surrounding air (see the upper, uncovered part of the leaf in the Fig. 1).

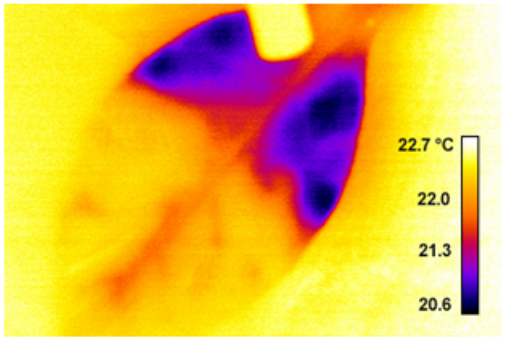

Fig. 1. Thermoimage of detached tobacco leaf made by thermal imaging Varioscan 3200 ST. The temperature changes are represented by false color. The upper part of tobacco leaf was covered by Vazeline. Spatial resolution of the thermoimage is 0.22 mm, temperature resolution in the picture is 0.03 °C. (For interpretation of the references to color in this figure legend, the reader is referred to the web version of the article.)

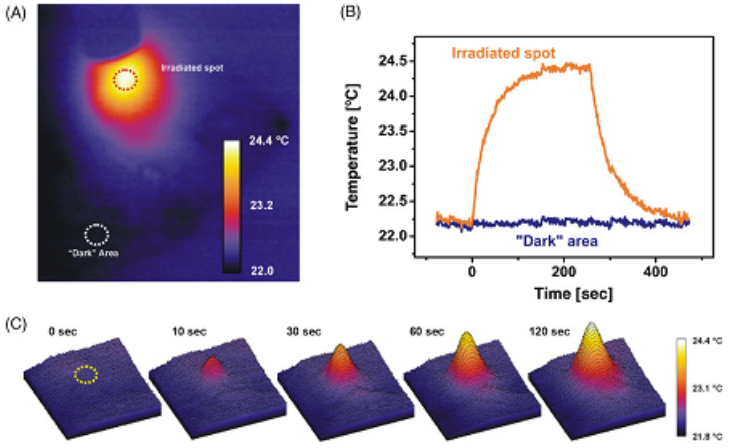

Fig. 2. Light-induced temperature increase of leaf surface. (A) Typical thermoimage of a leaf irradiated with blue actinic light (927 μM photons of PAR m^{-2} s^{-1}). The positions of irradiated and dark spots are marked on the picture by circles. (B) Characteristic time course of light-induced temperature increase. The values of these curves represent the mean temperatures calculated from the irradiated (orange line) or dark circular area (blue line) with diameter of 10 pixels in the central part of irradiated and dark spot. (C) 3D picture of temperature increase profile of leaf surface for irradiated spot of light at the indicated times after the onset of light. (For interpretation of the references to color in this figure legend, the reader is referred to the web version of the article.)

Irradiation of tobacco leaves caused increase in the temperature of the irradiated spot in comparison to the non-irradiated part of the leaf (Fig. 2A). A spatial heating profile during this temperature increase is presented for a period of 2 min after light onset (see Fig. 2C), which shows gradual increase in the temperature of the irradiated spot with diameter of about 0.8 cm (Fig. 2C). There is also a small increase outside the irradiated spot caused by lateral conduction of heat from the irradiated spot, which was, however, neglected in our model. Therefore, our model has considered only two vertical heat fluxes: (1) to the surrounding boundary layer of air above leaf surface; (2) the leaf tissue below irradiated spot as we have assumed absorption of all irradiation in the thin upper layer of leaf visible by the thermocamera. The leaf thickness has been than taken as the layer for vertical heat diffusion in the leaf below irradiated spot. Considering thickness of the boundary layer, as it is influenced by the leaf topography (Stokes et al., 2006), and changes along the leaf (Roth-Nebelsick, 2001), the position of the irradiated spot was kept the same for all experiments (about 2 cm from the leaf edge).

The kinetics of temperature increase of the irradiated spot is presented in Fig. 2B together with temperature changes in the non-irradiated parts of the leaf. It can be seen, that steady state temperatures are reached in about 1–2 min (Fig. 2B), whose values were dependent on light intensity (Fig. 3). The time necessary for reaching steady state temperatures of the irradiated spot is close to the previously obtained results for Vaseline covered leaves (see, e.g. Bajons et al., 2005). The non-irradiated part of the leaf did not reveal any significant increase in temperature after light onset (Figs. 2B and 3). This result indicates that irradiation does not affect the non-irradiated parts of the leaf, which are far enough from the irradiated spot (see the position of the dark area in Fig. 2A). The application of a saturating light pulse (necessary for calculation of the F_M' level of variable Chl a fluorescence, see Section 2) induced an additional temperature increase in the irradiated spot without affecting the surrounding area (Fig. 3). It can also be seen (Fig. 3) that 3 min in dark was enough for re-cooling of the irradiated spot to the former temperature before irradiation. Therefore, this period was then used between two subsequent irradiancies.

To explore the role of photosynthetic efficiency on light-induced temperature increase we exposed leaves to excessive irradiance. This treatment reduced the efficiency of photosystem II photochemistry and amplified non-photochemical utilization of light leading to increased NPQ. Fig. 4 shows that 6 h long exposure of tobacco leaves to about 1300 μM photons m^{-2} s^{-1} PAR increases NPQ for all used irradiancies as deduced from quenching of maximal fluorescence – F_M' (see insert in the Fig. 4). There were no changes in the steady state fluorescence level (F_t) between the quenched and the control samples (see, e.g. fluorescence induction curve for 512 μM photons m^{-2} s^{-1} in the insert of Fig. 4). Thus the energy consumed in the form of fluorescence emission was the same for control and quenched leaves. On the other hand, the effec-

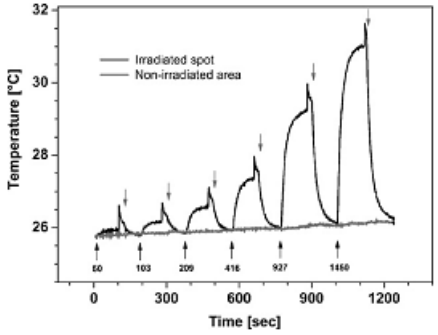

Fig. 3. Light intensity dependence of leaf temperature increase. Black and grey lines represent the mean value of temperature from the circular irradiated spot and dark area, respectively. The upward arrows show the onset of actinic light illuminated with the intensities (in μM photons m^{-2} s^{-1}) defined by the numbers below the arrows. The downward arrows show the termination of actinic illumination. The saturating pulse of 800 ms length and 6000 μM photons m^{-2} s^{-1} intensity was also applied before the end of each illumination as shown by the sharp temperature increase.

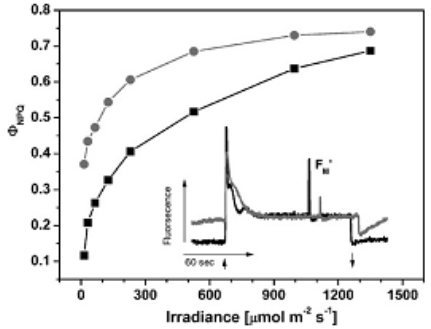

Fig. 4. Leaf intensity dependence of non-photochemical quenching after long-time exposure of tobacco leaves to high irradiancy. The experiment was performed in control leaves without preillumination (squares) and quenched leaves exposed to 1300 μM photons of PAR m^{-2} s^{-1} for 6 h (circles). The insert shows typical induction of fluorescence at 512 μM photons of PAR m^{-2} s^{-1} for control (black line) and quenched leaves (grey line). The time of actinic light application (termination) is marked by up arrow (down arrow), F_M' notes on the values of maximal fluorescence for light adapted state.

tive quantum yield of PSII photochemistry decreased to a similar extent (Fig. 5) as NPQ did. This lower efficiency of PSII photochemistry in the quenched samples was caused by the increased NPQ. All these results together have indicated that lower extent of energy consumption by photosynthesis resulted in increased dissipation of absorbed light energy into heat and not in the stimulation of other waste processes, e.g. variable Chl a fluorescence.

We have also found a small but reproducible increase in the temperature of the irradiated spot in the quenched leaves with higher NPQ relative to the control ones (Fig. 6A). To explore this result, we have applied the energy balance equation of leaves (see, e.g. Jones, 1992, 2004a). Based on this equation, we have developed a simple theoretical model of energy fluxes in leaves in the absence of evaporative cooling by taking into account the irradiation induced increase in the heat content, and its reduction due to conduction of heat from the irradiated spot and consumption in photosynthesis (see Section 2).

The efficiency of PSII photochemistry in the control and quenched samples have been used as input parameter of the

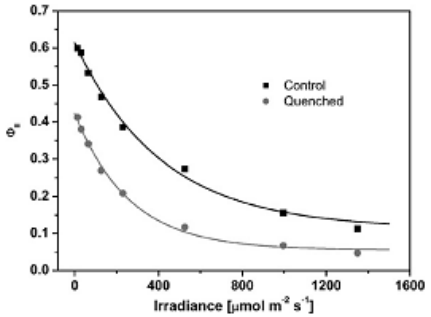

Fig. 5. Light intensity dependence of the efficiency of photosystem II photochemistry (Φ_{II}). The measurements were performed with leaves exposed to 1300 μM photons of PAR m^{-2} s^{-1} for 6 h (squares) and with control leaves without preillumination (circle). The continual lines show the fitting by a single exponential function whose parameters are listed in Table 1.

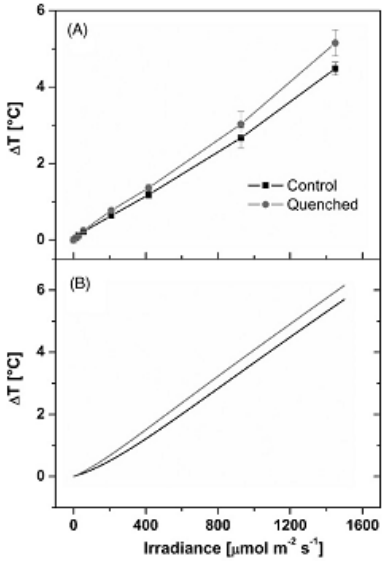

Fig. 6. The light intensity dependence of leaf temperature increase. The temperature difference was obtained for the irradiated spot in comparison to the dark area. Experimental data in (A) represent average and S.D. from 6 measurements for control (squares) and quenched leaves (circle). Theoretical curves in panel B were obtained by simulation based on the energy balance equation using the experimental Φ_{II} values (shown in Fig. 5) as input parameters of ΔT calculation (see Section 2).

model calculations. The experimental curves characterizing the light dependence of Φ_{II} were approximated by a simple exponential function $\Phi_{II}(I) = A_1 \exp(-I/t_1) + y_0$ where A_1, t_1 and y_0 are formal parameters, and I is the used irradiancy (see Fig. 5). The best fit parameters of the $\Phi_{II}(I)$ function (see Table 1.) have been used for calculation of Φ_{II} for all irradiancies between 0 and 1400 μM photons m^{-2} s^{-1} of PAR. These values were then used for calculation of temperature increase (ΔT) by Eq. (6), in the quenched and control leaves (Fig. 6B). The data show that even this very simple model is able to predict very well the small increase of leaf heating at a given irradiancy (Fig. 6B) caused by reduction in photosynthetic efficiency (Fig. 5B). This is in line with the experimental results showing similar extent of temperature increase in the quenched leaves (Fig. 6A), and confirm the applicability of our theoretical approach based on the energy balance equation.

For further explorations of light-induced heating of leaves, we have defined the efficiency of light dissipation into the heat – Φ_D. Its values were calculated according to our model with Φ_{II} as input

Table 1
Parameters describing the light intensity the light intensity dependence of the efficiency of PSII photochemistry (Φ_{II})

	Control	Quenched
y_0	0.113	0.055
A_1	0.501	0.368
t_1	413.7	260.4
χ^2	0.0003	0.0001

The experimentally determined curves shown in Fig. 5 were fitted with the function $\Phi_{II} = A_1 \exp(-I/t_1) + y_0$. A_1, t_1 and y_0 represent parameters of decay curve used for fitting of $\Phi_{II}(I)$ dependence for control and quenched sample, I is used irradiancy. χ^2 value was minimized during fitting procedure.

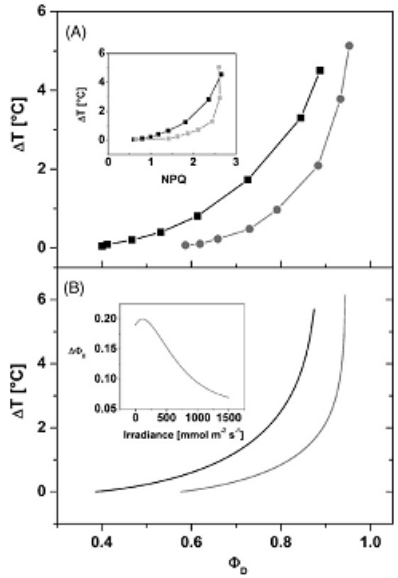

Fig. 7. Dependence of light-induced leaf temperature increase (ΔT) on the efficiency of light conversion to heat (Φ_D). (A) Experimentally obtained data for control (squares) and quenched (circle) leaves. The theoretical curves in (B) were calculated based on the energy balance equation using the experimental Φ_{II} values (shown in Fig. 5) as the input parameters of ΔT calculation (see Section 2). Inset in (A) shows dependence of ΔT on non-photochemical quenching – NPQ. Insert in panel B shows the difference in the efficiency of the quantum efficiency of photosystem II photochemistry between control and quenched sample $\Delta\Phi_{II}$ calculated from Eq. (10).

parameter (see Section 2) by Eq. (9). Similar approach characterizing energy fluxes into heat and into photosynthesis have been already defined based on Chl a fluorescence measurements (Kramer et al., 2004, Hendrickson et al., 2004, Porcar-Castell et al., 2006). Kramer et al. (2004) have derived fluxes of absorbed energy into photochemistry of photosystem II – Φ_{II}, and also two competing energy fluxes into heat (Φ_{NPQ} and Φ_{NO}, see Section 2 for details). We assumed that both energy fluxes into heat (Φ_{NPQ} and Φ_{NO}) result in temperature increase and thus we defined the efficiency of light dissipation into heat as $\Phi_D = \Phi_{NPQ} + \Phi_{NO}$. The sum of the dissipation yields (i.e. Φ_{II}, Φ_{NPQ} and Φ_{NO}) has been postulated to be unity both in our model and that of Kramer et al. (2004). This allowed us to compare experimental results based on Kramer's parameters obtained from fluorescence measurements and the results calculated from our theoretical model.

Fig. 7 shows the dependence of the observed leaf temperature increase on the efficiency of the light dissipation into heat (Φ_D) for experimental data (panel A) and model calculations (panel B). The control leaves had steeper temperature increase than the quenched ones (Fig. 7A) for both the experimental and theoretical results. It is interesting to note that the same value of Φ_D results in higher temperature increase in control then in quenched leaves. Therefore, there is a higher extent of energy flux into heat at given Φ_D in control leaves even though the absolute amount of energy wasted as heat is slightly higher for quenched leaves (Fig. 6).

It is also obvious that the correlation between leaf temperature increase and efficiency of energy dissipation (Φ_D) to heat is not linear (Fig. 7A and insert of the Fig. 7A). This is because Φ_D and NPQ are limited in their values – they cannot be higher than the maximal efficiency of light dissipation (e.g. 100%) and thus they just slowly approach this limiting level of efficiency of dissipation with increasing irradiancy. Our results show for the first time the correlation between heat dissipation efficiency (characterized by Φ_D or NPQ) and actual heating of leaves represented by temperature increase (see inset of Fig. 7A). This is an important phenomenon since one of these parameters, NPQ, reflects a physiological mechanism involved in the regulation of excessive irradiation absorbed by PSII into heat (see, e.g. for details Horton and Ruban, 2005 for review). However, the different dependence of temperature increase on NPQ (or Φ_D) in control and quenched leaves would not be expected if the heat dissipation mechanism would be identical for both of them. Since long exposure to excessive radiation could result in the reduction of leaf absorbance due to e.g. chloroplast movement (see, e.g Kasahara et al., 2002) we have checked the possible role of this phenomenon in the $\Delta T(\Phi_D)$ dependence. However, we have not been able to simulate the same $\Delta T(\Phi_D)$ curve for control and quenched leaves by any reduction of leaf absorbance (data not shown). Therefore, the observed difference of $\Delta T(\Phi_D)$ in control and quenched leaves is most likely related to different light dependent changes of Φ_{II}. This suggestion has been confirmed on the basis of model calculations, where the $\Delta\Phi_{II}$ difference between the control and quenched leaves can be calculated by equation (10), resulting in different $\Delta T(\Phi_D)$ for the control and quenched leaves (Fig. 7B). It can be also seen that with increasing light irradiancies $\Delta\Phi_{II}$ decreases (see insert of the Fig. 7B). This can be explained by decreasing differences of Φ_D for control and quenched leaves, during increasing irradiancies (Fig. 4).

However, the different dependence of temperature increase on NPQ (or Φ_D) in control and quenched leaves can be caused not only by Φ_{II} reduction, but also by acceleration of some additional energy consuming processes outside of PSII in quenched leaves (e.g. cyclic electron transport around PSI, see, e.g. Johnson, 2005 for recent review). Such acceleration of alternative pathways of plastoquinone reduction via cyclic electron transport around PSI by excessive irradiation has been shown by previous results (Endo et al., 1999, Quiles and Lopez, 2004). This effect has been shown to induce the increase of the F_0' level after termination of light (Burrows et al., 1998, Field et al., 1998), which was also observed in our experiments, and notably the effect was more pronounced for quenched than for the control leaves (see insert in the Fig. 4). The same amplification of cyclic electron flow around PSI has been recently shown also for *Tobacco* plants growing at higher irradiancy (Miyake et al., 2005) and its origin has been already confirmed by mutants (Yamamoto and Miyake, 2007). However, the precise testing of the cyclic electron flow around PSI in the view of the different temperature increase after irradiation needs more complex model of energy balance in leaf.

4. Conclusions

Our sensitive thermal imaging measurements have demonstrated the correlation between the extent of NPQ and light-induced temperature increase in tobacco leaves, which results in higher leaf temperature increase in the presence of higher extent of NPQ. We have also found that the correlation between leaf heating and the efficiency of light dissipation is different for control and quenched leaves. This observation can be explained by a simple model of leaf energy balance assuming light intensity dependent reduction in the efficiency of PSII photochemistry. However, a more detailed explanation of this effect requires future research.

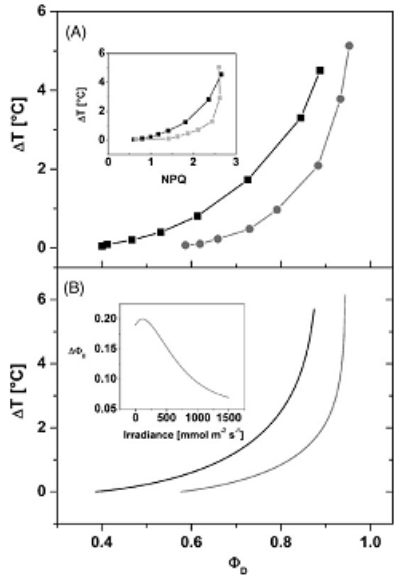

Fig. 7. Dependence of light-induced leaf temperature increase (ΔT) on the efficiency of light conversion to heat (Φ_D). (A) Experimentally obtained data for control (squares) and quenched (circle) leaves. The theoretical curves in (B) were calculated based on the energy balance equation using the experimental Φ_{II} values (shown in Fig. 5) as the input parameters of ΔT calculation (see Section 2). Inset in (A) shows dependence of ΔT on non-photochemical quenching – NPQ. Insert in panel B shows the difference in the efficiency of the quantum efficiency of photosystem II photochemistry between control and quenched sample $\Delta\Phi_{II}$ calculated from Eq. (10).

parameter (see Section 2) by Eq. (9). Similar approach characterizing energy fluxes into heat and into photosynthesis have been already defined based on Chl a fluorescence measurements (Kramer et al., 2004, Hendrickson et al., 2004, Porcar-Castell et al., 2006). Kramer et al. (2004) have derived fluxes of absorbed energy into photochemistry of photosystem II – Φ_{II}, and also two competing energy fluxes into heat (Φ_{NPQ} and Φ_{NO}, see Section 2 for details). We assumed that both energy fluxes into heat (Φ_{NPQ} and Φ_{NO}) result in temperature increase and thus we defined the efficiency of light dissipation into heat as $\Phi_D = \Phi_{NPQ} + \Phi_{NO}$. The sum of the dissipation yields (i.e. Φ_{II}, Φ_{NPQ} and Φ_{NO}) has been postulated to be unity both in our model and that of Kramer et al. (2004). This allowed us to compare experimental results based on Kramer's parameters obtained from fluorescence measurements and the results calculated from our theoretical model.

Fig. 7 shows the dependence of the observed leaf temperature increase on the efficiency of the light dissipation into heat (Φ_D) for experimental data (panel A) and model calculations (panel B). The control leaves had steeper temperature increase than the quenched ones (Fig. 7A) for both the experimental and theoretical results. It is interesting to note that the same value of Φ_D results in higher temperature increase in control then in quenched leaves. Therefore, there is a higher extent of energy flux into heat at given Φ_D in control leaves even though the absolute amount of energy wasted as heat is slightly higher for quenched leaves (Fig. 6).

It is also obvious that the correlation between leaf temperature increase and efficiency of energy dissipation (Φ_D) to heat is not linear (Fig. 7A and insert of the Fig. 7A). This is because Φ_D and NPQ are limited in their values – they cannot be higher than the maximal efficiency of light dissipation (e.g. 100%) and thus they just slowly approach this limiting level of efficiency of dissipation with increasing irradiancy. Our results show for the first time the correlation between heat dissipation efficiency (characterized by Φ_D or NPQ) and actual heating of leaves represented by temperature increase (see inset of Fig. 7A). This is an important phenomenon since one of these parameters, NPQ, reflects a physiological mechanism involved in the regulation of excessive irradiation absorbed by PSII into heat (see, e.g. for details Horton and Ruban, 2005 for review). However, the different dependence of temperature increase on NPQ (or Φ_D) in control and quenched leaves would not be expected if the heat dissipation mechanism would be identical for both of them. Since long exposure to excessive radiation could result in the reduction of leaf absorbance due to e.g. chloroplast movement (see, e.g Kasahara et al., 2002) we have checked the possible role of this phenomenon in the $\Delta T(\Phi_D)$ dependence. However, we have not been able to simulate the same $\Delta T(\Phi_D)$ curve for control and quenched leaves by any reduction of leaf absorbance (data not shown). Therefore, the observed difference of $\Delta T(\Phi_D)$ in control and quenched leaves is most likely related to different light dependent changes of Φ_{II}. This suggestion has been confirmed on the basis of model calculations, where the $\Delta\Phi_{II}$ difference between the control and quenched leaves can be calculated by equation (10), resulting in different $\Delta T(\Phi_D)$ for the control and quenched leaves (Fig. 7B). It can be also seen that with increasing light irradiancies $\Delta\Phi_{II}$ decreases (see insert of the Fig. 7B). This can be explained by decreasing differences of Φ_D for control and quenched leaves, during increasing irradiancies (Fig. 4).

However, the different dependence of temperature increase on NPQ (or Φ_D) in control and quenched leaves can be caused not only by Φ_{II} reduction, but also by acceleration of some additional energy consuming processes outside of PSII in quenched leaves (e.g. cyclic electron transport around PSI, see, e.g. Johnson, 2005 for recent review). Such acceleration of alternative pathways of plastoquinone reduction via cyclic electron transport around PSI by excessive irradiation has been shown by previous results (Endo et al., 1999, Quiles and Lopez, 2004). This effect has been shown to induce the increase of the F_0' level after termination of light (Burrows et al., 1998, Field et al., 1998), which was also observed in our experiments, and notably the effect was more pronounced for quenched than for the control leaves (see insert in the Fig. 4). The same amplification of cyclic electron flow around PSI has been recently shown also for *Tobacco* plants growing at higher irradiancy (Miyake et al., 2005) and its origin has been already confirmed by mutants (Yamamoto and Miyake, 2007). However, the precise testing of the cyclic electron flow around PSI in the view of the different temperature increase after irradiation needs more complex model of energy balance in leaf.

4. Conclusions

Our sensitive thermal imaging measurements have demonstrated the correlation between the extent of NPQ and light-induced temperature increase in tobacco leaves, which results in higher leaf temperature increase in the presence of higher extent of NPQ. We have also found that the correlation between leaf heating and the efficiency of light dissipation is different for control and quenched leaves. This observation can be explained by a simple model of leaf energy balance assuming light intensity dependent reduction in the efficiency of PSII photochemistry. However, a more detailed explanation of this effect requires future research.

Acknowledgements

This work has been supported by EU grant MRTN-CT-2003-505069 (INTRO 2 – *Interdisciplinary Network for Training and Research on Photosystem 2*), the Hungarian Wheat Consortium, and also by the Ministry of Education, Youth and Sports (research concepts MSM 6198959215). The research in the Institute of Microbiology (Academy of Sciences of the Czech Republic, Třeboň) has been supported by the Grant Agency of Czech Republic (GACR 206-05-0335) and by research concept AV0Z50200510. We would like to thanks to Vladimíra Hlaváčková (UP Olomouc) for providing tobacco plants.

References

Abramoff, M.D., Magelhaes, P.J., Ram, S.J., 2004. Image processing with ImageJ. Biophotonics Int. 11 (7), 36–42.

Bajons, P., Klinger, G., Schlosser, V., 2005. Determination of stomatal conductance by means of infrared thermography. Infrared Phys. Technol. 46, 429–439.

Bults, G., Nordal, P.E., Kanstad, S.O., 1982. In vivo studies of gross photosynthesis in attached leaves by means of photothermal radiometry. Biochim. Biophys. Acta 682, 234–237.

Burrows, P.A., Sazanov, L.A., Svab, Z., Maliga, P., Nixon, P.J., 1998. Identification of a functional respiratory complex in chloroplasts through analysis of tobacco mutants containing disrupted plastid ndh genes. EMBO J. 17, 868–876.

Cambell, G.S., Norman, J.M., 1998. An Introduction to Environmental Biophysics. Springer, Netherlands.

Chaerle, L., Hagenbeek, D., De Bruyne, E., Valcke, R., Van der Straeten, D., 2004. Thermal and chlorophyll-fluorescence imaging distinguish plant-pathogen interactions at an early stage. Plant Cell Physiol. 45, 887–896.

Cohen, Y., Alchanatis, V., Meron, M., Saranga, Y., Tsipris, J., 2005. Estimation of leaf water potential by thermal imagery and spatial analysis. J. Exp. Bot. 56, 1843–1852.

Cui, M., Vogelmann, T.C., Smith, W.K., 1991. Chlorophyll and light gradients in sun and shade leaves of *Spinacia oleracea*. Plant Cell Environ. 14, 493–500.

Delosme, R., 2003. On some aspects of photosynthesis revealed by photoacoustic studies, a critical evaluation. Photosynth. Res. 76, 289–301.

Driesenaar, A.R.J., Schreiber, U., Malkin, S., 1994. The use of photothermal radiometry in assessing leaf photosynthesis. 2. Correlation of energy-storage to photosystem-ii fluorescence parameters. Photosynth. Res. 40, 45–53.

Endo, T., Shikanai, T., Takabayashi, A., Asada, K., Sato, F., 1999. The role of chloroplastic NAD(P)H dehydrogenase in photoprotection. FEBS Lett. 457, 5–8.

Field, T.S., Nedbal, L., Ort, D.R., 1998. Nonphotochemical reduction of the plastoquinone pool in sunflower leaves originates from chlororespiration. Plant Physiol. 116, 1209–1218.

Genty, B., Briantais, J.M., Baker, N.R., 1989. The relationship between the quantum yield of photosynthetic electron-transport and quenching of chlorophyll fluorescence. Biochim. Biophys. Acta 990, 87–92.

Hendrickson, L., Furbank, R.T., Chow, W.S., 2004. A simple alternative approach to assessing the fate of absorbed light energy using chlorophyll fluorescence. Photosynth. Res. 82, 73–81.

Horton, P., Ruban, A., 2005. Molecular design of the photosystem II light-harvesting antenna, photosynthesis and photoprotection. J. Exp. Bot. 56, 365–373.

Horton, P., Wentworth, M., Ruban, A., 2005. Control of the light harvesting function of chloroplast membranes: the LHCII-aggregation model for non-photochemical quenching. FEBS Lett. 579, 4201–4206.

Johnson, G.N., 2005. Cyclic electron transport in C-3 plants: fact or artefact? J. Exp. Bot. 56, 407–416.

Jones, H.G., 1992. Plants and Microclimate, second ed. Cambridge University Press, Cambridge, Massachusetts.

Jones, H.G., 2004a. Application of thermal imaging and infrared sensing in plant physiology and ecophysiology. *In* Advances in Botanical Research Incorporating Advances in Plant Pathology. Advances in Botanical Research Incorporating Advances in Plant Pathology, 41. Academic Press Ltd., London, pp 107–163.

Jones, H.G., 2004b. Irrigation scheduling: advantages and pitfalls of plant-based methods. J. Exp. Bot. 55, 2427–2436.

Jones, H.G., Archer, N., Rotenberg, E., Casa, R., 2003. Radiation measurement for plant ecophysiology. J. Exp. Bot. 54, 879–889.

Jones, H.G., Stoll, M., Santos, T., de Sousa, C., Chaves, M.M., Grant, O.M., 2002. Use of infrared thermography for monitoring stomatal closure in the field: application to grapevine. J. Exp. Bot. 53, 2249–2260.

Kanstad, S.O., Cahen, D., Malkin, S., 1983. Simultaneous detection of photosynthetic energy-storage and oxygen evolution in leaves by photothermal radiometry and photoacoustics. Biochim. Biophys. Acta 722, 182–189.

Kasahara, M., Kagawa, T., Oikawa, K., Suetsugu, N., Miyao, M., Wada, M., 2002. Chloroplast avoidance movement reduces photodamage in plants. Nature 420, 829–832.

Kramer, D.M., Johnson, G., Kiirats, O., Edwards, G.E., 2004. New fluorescence parameters for the determination of Q(A) redox state and excitation energy fluxes. Photosynth. Res. 79, 209–218.

Lamprecht, I., Schmolz, E., Blanco, L., Romero, C.M., 2002. Flower ovens: thermal investigations on heat producing plants. Thermoch. Acta 391, 107–118.

Leinonen, I., Grant, O.M., Tagliavia, C.P.P., Chaves, M.M., Jones, H.G., 2006. Estimating stomatal conductance with thermal imagery. Plant Cell Environ. 29, 1508–1518.

Malkin, S., Schreiber, U., Jansen, M., Canaani, O., Shalgi, E., Cahen, D., 1991. The use of photothermal radiometry in assessing leaf photosynthesis. 1. General-properties and correlation of energy-storage to P-700 redox state. Photosynth. Res. 29, 87–96.

Maxwell, K., Johnson, G.N., 2000. Chlorophyll fluorescence—a practical guide. J. Exp. Bot. 51, 659–668.

Merlot, S., Mustilli, A.C., Genty, B., North, H., Lefebvre, V., Sotta, B., Vavasseur, A., Giraudat, J., 2002. Use of infrared thermal imaging to isolate Arabidopsis mutants defective in stomatal regulation. Plant J. 30, 601–609.

Miyake, Ch., Horiguchi, S., Makino, A., Shinzaki, Y., Yamamoto, H., Tomizawa, K., 2005. Effects of light intensity on cyclic electron flow around PS I and its relation to non-photochemical quenching of chl fluorescence in tobacco leaves. Plant Cell Physiol. 46, 1819–1830.

Nordal, P., Kanstad, S.O., 1981. Visible-light spectroscopy by photothermal radiometry using an incoherent source. Appl. Phys. Lett. 38, 486–488.

Omasa, K., Takayama, K., 2003. Simultaneous measurement of stomatal conductance, non-photochemical quenching, and photochemical yield of photosystem II in intact leaves by thermal and chlorophyll fluorescence imaging. Plant Cell Physiol. 44, 1290–1300.

Porcar-Castell, A., Back, J., Juurola, E., Hari, P., 2006. Dynamics of the energy flow through photosystem II under changing light conditions: a model approach. Funct. Plant Biol. 33, 229–239.

Quiles, M.J., Lopez, N.I., 2004. Photoinhibition of photosystems I and II induced by exposure to high light intensity during oat plant growth - Effects on the chloroplast NADH dehydrogenase complex. Plant Sci. 166, 815–823.

Rasband, W.S., 1997–2008. ImageJ. US National Institutes of Health, Bethesda, Maryland, USA, http://rsb.info.nih.gov/ij/.

Roth-Nebelsick, A., 2001. Computer-based analysis of steady-state and transient heat transfer of small-sized leaves by free and mixed convection. Plant Cell Environ. 24, 631–640.

Schuepp, P.H., 1993. Tansley review no 59 leaf boundary-layers. New Phytol. 125, 477–507.

Stokes, V.J., Morecroft, M.D., Morison, J.I.L., 2006. Boundary layer conductance for contrasting leaf shapes in a deciduous broadleaved forest canopy. Agric. Forest Meteor. 139, 40–54.

West, J.D., Peak, D., Peterson, J.Q., Mott, K.A., 2005. Dynamics of stomatal patches for a single surface of *Xanthium strumarium* L. leaves observed with fluorescence and thermal images. Plant Cell Environ. 28, 633–641.

Yamamoto, H., Miyake, C., 2007. Overexpression of ferredoxin in tobacco chloroplasts stimulates Cyclic Electron Flow around Photosystem I (CEF-PSI) and enhances non-photochemical quenching (NPQ) of Chl fluorescence. Photos. Res. 91, 242–1242.